

# The Occurrence and Architecture of Exoplanetary Systems

JOSHUA N. WINN

*Department of Physics, Massachusetts Institute of Technology,  
Cambridge, Massachusetts, 02139; email: jwinn@mit.edu*

DANIEL C. FABRYCKY

*Department of Astronomy and Astrophysics, University of Chicago,  
Chicago, IL, 60637; email: fabrycky@uchicago.edu*

## Key Words

exoplanets, extrasolar planets, orbital properties, planet formation

## Abstract

The basic geometry of the Solar System—the shapes, spacings, and orientations of the planetary orbits—has long been a subject of fascination as well as inspiration for planet-formation theories. For exoplanetary systems, those same properties have only recently come into focus. Here we review our current knowledge of the occurrence of planets around other stars, their orbital distances and eccentricities, the orbital spacings and mutual inclinations in multiplanet systems, the orientation of the host star’s rotation axis, and the properties of planets in binary-star systems.

## 1 INTRODUCTION

Over the centuries, astronomers gradually became aware of the following properties of the Solar System:

- The Sun has eight planets, with the four smaller planets ( $R_p = 0.4\text{--}1.0 R_\oplus$ ) interior to the four larger planets ( $3.9\text{--}11.2 R_\oplus$ ).
- The orbits are all nearly circular, with a mean eccentricity of 0.06 and individual eccentricities ranging from 0.0068–0.21.
- The orbits are nearly aligned, with a root-mean-squared inclination of  $1^\circ.9$  relative to the plane defined by the total angular momentum of the Solar System (the “invariable plane”), and individual inclinations ranging from  $0^\circ.33\text{--}6^\circ.3$ .
- The Sun’s rotational angular momentum is much smaller than the orbital angular momentum of the planets ( $L_\odot/L_{\text{orb}} \approx 0.5\%$ ).
- The Sun’s equator is tilted by  $6^\circ.0$  relative to the invariable plane.
- The sizes of neighboring orbits have ratios in the range of 1.4–3.4.

These regularities have long been recognized as important clues about the formation of the Solar System. Isaac Newton realized that the Solar System is more orderly than required by the laws of motion and took this as evidence for God’s hand in creation. Pierre-Simon Laplace was inspired by the same facts to devise a mechanistic theory for the formation of the Solar System. Since then, it became traditional to begin any article on the formation of the Solar System with a list of observations similar to the one provided above.

Many authors of such articles have expressed a wish to have the same type of information for other planetary systems. In a representative example, Williams & Cremin (1968) wrote, “It is difficult to decide whether all the major properties of the Solar System have been included above, or indeed whether all the above properties are essential properties of any system formed under the same conditions as the Solar System. This is because only one Solar System is known to exist and so it is impossible to distinguish between phenomena that must come about as a direct consequence of some established law and phenomena that come about as a result of unlikely accidents.”

In the past few decades these wishes have begun to be fulfilled. In this review, we have attempted to construct an exoplanetary version of the traditional list of elementary properties of the Solar System. Our motivation is mainly empirical. The measurement of exoplanetary parameters is taken to be an end unto itself. Theories to explain the values of those parameters are discussed but not comprehensively. For brevity, we have also resisted the temptation to review the history of exoplanetary science or the techniques of exoplanet detection.<sup>1</sup> Our main concern is the geometry of exoplanetary systems—the parameters that Newton and Laplace would have immediately appreciated—as opposed to atmospheres, interior compositions, and other aspects of post-Apollo planetary science. However, we have added a parameter to the list that may have surprised Newton and Laplace: the number of host stars, which need not be one.

This article is organized as follows. Section 2 answers the first question our predecessors would have asked: How common, or rare, are planets around other stars? Section 3 discusses the sizes and shapes of individual planetary orbits. This is followed in section 4 by a discussion of multiplanet systems, particularly their orbital spacings and mutual inclinations. Section 5 considers the rotation of the host star, and section 6 considers planets in binary-star systems. Finally, Section 7 summarizes the exoplanetary situation, comments on the implications for planet-formation theory, and discusses the future prospects for improving our understanding of exoplanetary architecture.

## 2 OCCURRENCE RATE

No simple physical principle tells us whether planets should be rare or common. Before the discovery of exoplanets, there was ample room for speculation. Monistic planet-formation theories, in which planet and star formation are closely related, predicted that planets should be ubiquitous; an example was Laplace’s nebular theory, in which planets condense from gaseous rings ejected from a spinning protostar. In contrast, dualistic theories held that planets arise from events that are completely distinct from star formation, and in many such theories the events were extremely unlikely. An example was the tidal theory in which planets condense from material stripped away from a star during a chance encounter with another star. This was predicted to occur with a probability of  $\sim 10^{-10}$  for a given star,

---

<sup>1</sup>For history, see the collection of articles edited by Lissauer (2012). For detection techniques, see Seager (2011) or Wright & Gaudi (2013). For theory, see Ford (2014).

although Jeans (1942) managed to increase the odds to  $\sim 0.1$  by allowing the encounter to happen during pre-main-sequence contraction.

Modern surveys using the Doppler, transit, and microlensing techniques have shown that planets are prevalent. The probability that a random star has a planet is of order unity for the stars that have been searched most thoroughly: main-sequence dwarfs with masses  $0.5\text{--}1.2 M_{\odot}$ . Monistic theories have prevailed, including the currently favored theory of planet formation in which planets build up from small particles within the gaseous disks that surround all young stars.

The occurrence rate is the mean number of planets per star having properties (such as mass and orbital distance) within a specified range. The basic idea is to count the number of detected planets with the stipulated properties and divide by the effective number of stars in the survey for which such a planet could have been detected. The word “effective” reminds us that it is not always clear-cut whether or not a planet could have been detected; in such cases one must sum the individual detection probabilities for each star.

Accurate measurement of occurrence rates requires a large sample of stars that have been searched for planets and a good understanding of the selection effects that favor the discovery of certain types of planets. Because of these effects there can be major differences between the observed sample and a truly representative sample of planets. This is illustrated in Figs. 1 and 2. Fig. 1 shows the estimated masses and orbital distances of most of the known exoplanets, labeled according to detection technique. Although this provides a useful overview, it is misleading because it takes no account of selection effects. Fig. 2 shows a simulated volume-limited sample of planets around the nearest thousand FGK dwarfs; the simulation is based on measurements of planet occurrence rates that are described below.

Giant planets dominate the observed distribution, but smaller planets are far more numerous in the simulated volume-limited sample. What appears in the observed distribution to be a pile-up of hot Jupiters (a few hundred Earth masses at a few hundredths of an AU) has vanished in the volume-limited sample. In reality it is not clear that hot Jupiters form a separate population from the giant planets at somewhat larger orbital distances.

Table 1 gives some key results of selected studies. Before discussing these individual studies, we summarize the basic picture:

1. Nature seems to distinguish between planets and brown dwarfs. For orbital periods shorter than a few years, companions with masses between  $10$  and  $100 M_{\text{Jup}}$  are an order-of-magnitude rarer than less massive objects (Marcy & Butler 2000, Grether & Lineweaver 2006, Sahlmann et al. 2011). This is known as the brown dwarf desert.
2. Nature also seems to distinguish between giant planets and smaller planets, with a dividing line at a radius of approximately  $4 R_{\oplus}$  ( $0.4 R_{\text{Jup}}$ ) or a mass of approximately  $30 M_{\oplus}$  ( $0.1 M_{\text{Jup}}$ ). Giants are less abundant than smaller planets per unit  $\log R_p$  or  $\log M_p$ , within the period range that has been best investigated ( $P \lesssim 1$  year). Giants are also associated with a higher heavy-element abundance in the host star’s photosphere and a broader eccentricity distribution than smaller planets.
3. Giant planets with periods shorter than a few years are found around  $\approx 10\%$  of Sun-like stars, with a probability density nearly constant in  $\log P$  between 2–2000 days. Giants are rarely found with  $P < 2$  days.
4. Smaller planets ( $1\text{--}4 R_{\oplus}$ ) with  $P \lesssim 1$  year are found around approximately half of Sun-like stars, often in closely spaced multiplanet systems. The probability density

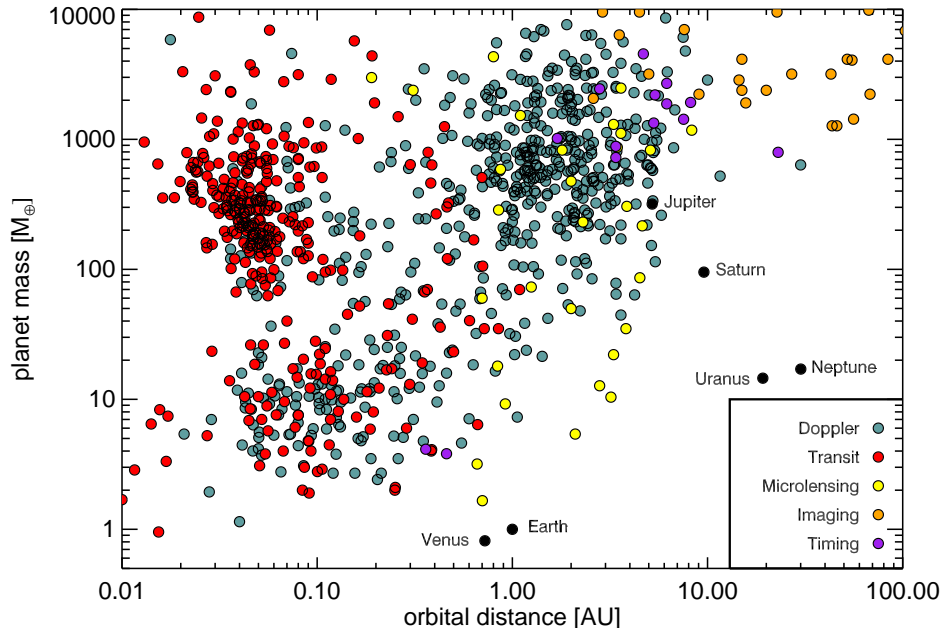


Figure 1 Approximate masses and orbital distances of known planets, based on an October 2014 query of the `exoplanets.eu` encyclopedia (Schneider et al. 2011). This plot does not consider selection biases and glosses over many important details. For Doppler planets, the plotted mass is really  $M_p \sin i$ . For imaging planets, the plotted mass is based on theoretical models relating the planet’s age, luminosity, and mass. With microlensing, the planet-to-star mass ratio is determined more directly than the planet mass. For microlensing and imaging planets, the plotted orbital distance is really the sky-projected orbital distance. For transiting planets, thousands of candidates identified by the *Kepler* mission are missing; these have unknown masses, but many of them are likely to be planets. For timing planets, many are dubious cases of circumbinary planets around evolved stars (see § 6.2).

is nearly constant in  $\log P$  between about 10 and 300 days. For  $P \lesssim 10$  days the occurrence rate declines sharply with decreasing period.

## 2.1 Doppler planets

Cumming et al. (2008) analyzed the results of a Doppler campaign in which nearly 600 FGKM stars were monitored for 8 years. They fitted a simple function to the inferred probability density for planets with mass  $> 100 M_\oplus$  and  $P < 5.5$  yr,

$$\frac{dN}{d \ln M_p d \ln P} \propto M_p^\alpha P^\beta, \quad (1)$$

and found  $\alpha = -0.31 \pm 0.20$ ,  $\beta = 0.26 \pm 0.10$ , and a normalization such that the occurrence rate for  $P < 5.5$  yr and  $M_p = 0.3\text{-}10 M_{\text{Jup}}$  is 10.5%. This function became a benchmark for many subsequent studies. Udry et al. (2003) and Cumming et al. (2008) found evidence for

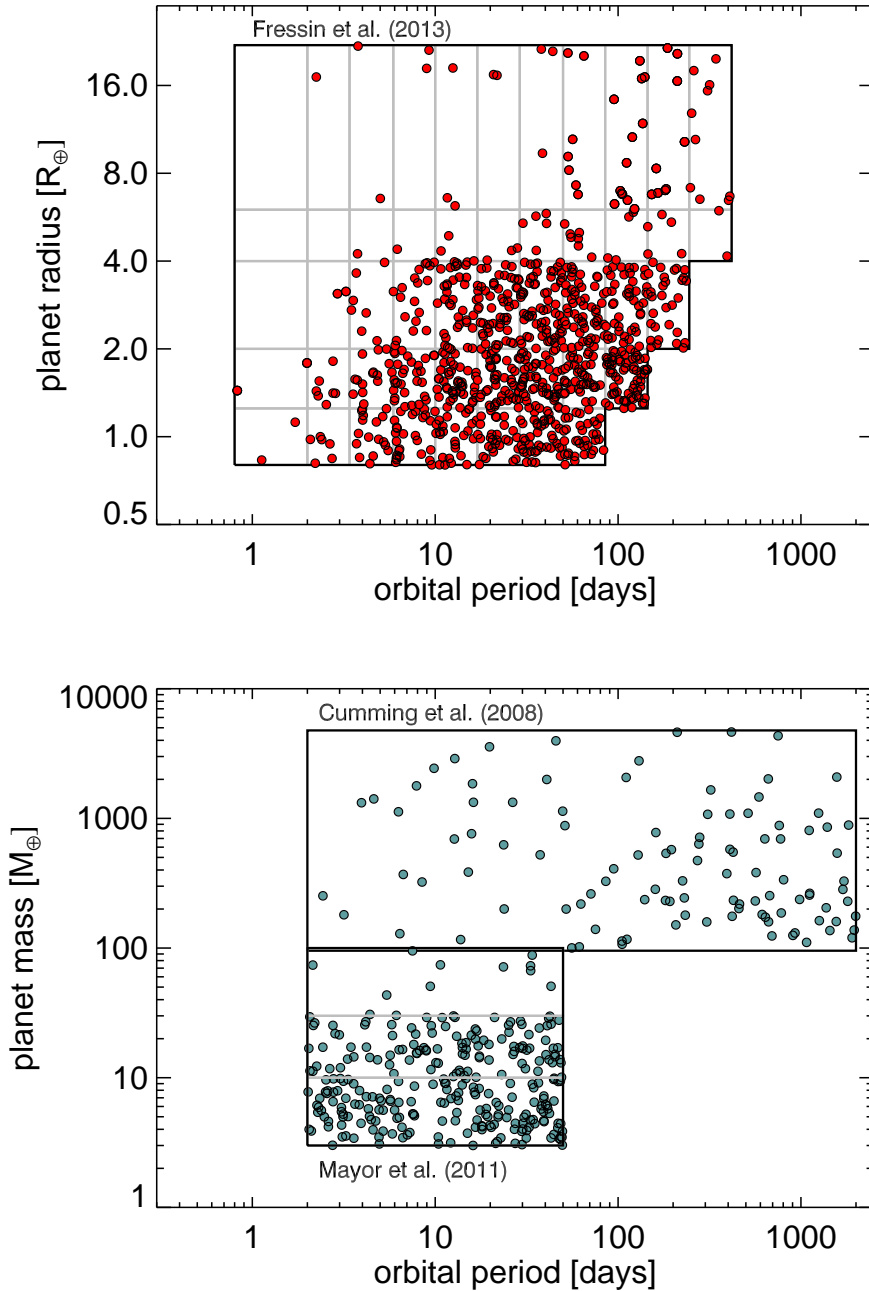


Figure 2 Properties of a hypothetical sample of exoplanets around the nearest thousand FGK dwarfs, based on measured planet occurrence rates. *Top.*—Sizes and periods, based on the analysis of *Kepler* data by Fressin et al. (2013). The grid indicates the size and period range corresponding to each element in the matrix of planet occurrence rates provided by those authors. *Bottom.*—Masses and periods, based on the Doppler results of Cumming et al. (2008) for larger planets and Mayor et al. (2011) for smaller planets.

Table 1. Planet occurrence rates around FGK stars

Study	Technique	Period range	Size range	Occurrence [%]
Wright et al. (2012)	Doppler	< 10 d	> 30 $M_{\oplus}$	$1.20 \pm 0.38$
Mayor et al. (2011)	Doppler	< 11 d	> 50 $M_{\oplus}$	$0.89 \pm 0.36$
Cumming et al. (2008)	Doppler	< 5.2 yr	>100 $M_{\oplus}$	$8.5 \pm 1.3$
		<100 d	>100 $M_{\oplus}$	$2.4 \pm 0.7$
Howard et al. (2010)	Doppler	<50 d	3–10 $M_{\oplus}$	$11.8^{+4.3}_{-3.5}$
		<50 d	10–30 $M_{\oplus}$	$6.5^{+3.0}_{-2.3}$
Mayor et al. (2011)	Doppler	<50 d	3–10 $M_{\oplus}$	$16.6 \pm 4.4$
		<50 d	10–30 $M_{\oplus}$	$11.1 \pm 2.4$
		<10 yr	>50 $M_{\oplus}$	$13.9 \pm 1.7$
Fressin et al. (2013)	Transit	<10 d	6–22 $R_{\oplus}$	$0.43 \pm 0.05$
		<85 d	0.8–1.25 $R_{\oplus}$	$16.6 \pm 3.6$
		<85 d	1.25–2 $R_{\oplus}$	$20.3 \pm 2.0$
		<85 d	2–4 $R_{\oplus}$	$19.9 \pm 1.2$
		<85 d	1.25–22 $R_{\oplus}$	$52.3 \pm 4.2$
Petigura et al. (2013)	Transit	5–100 d	1–2 $R_{\oplus}$	$26 \pm 3$
		5–100 d	8–16 $R_{\oplus}$	$1.6 \pm 0.4$

a few features in the period distribution that are not captured in Equation (1). Specifically, there appears to be a  $\approx 2\sigma$  excess of hot Jupiters, followed by a “period valley” of lower probability. There is also a sharper rise in probability as the period exceeds  $\approx 1$  year ( $a \gtrsim 1$  AU). This can be glimpsed in Figure 1, but is not modeled in Figure 2.

Howard et al. (2010) and Mayor et al. (2011) explored the domain of smaller planets with periods up to about 50 days, finding that such planets are more common than giants. Mayor et al. (2011) also revealed that small short-period planets frequently come in compact multiplanet systems, as later confirmed by the NASA *Kepler* mission (see § 2.2).

Doppler surveys also revealed that giant-planet occurrence is strongly associated with a high heavy-element abundance in the host star’s photosphere (Gonzalez 1997, Santos et al. 2004, Valenti & Fischer 2005). In contrast, small-planet occurrence is not associated with high metallicity in FGK dwarfs (Sousa et al. 2008, Buchhave et al. 2012). Likewise, the occurrence of stellar companions shows little or no correlation with metallicity (Carney et al. 2005, Raghavan et al. 2010, Grether & Lineweaver 2007), supporting the notion that giant planet formation is fundamentally different than binary-star formation.

The M dwarfs are more plentiful per cubic parsec than any other type of star, but they are more difficult to observe owing to their low luminosities and relatively complex spectra. One secure result is that they have fewer giant planets with  $P \lesssim 1$  year than FGK dwarfs (Butler et al. 2004, Endl et al. 2006, Johnson et al. 2007, Bonfils et al. 2013). In particular, Cumming et al. (2008) showed that if the scaling law in planetary mass and period of Equation (1) holds for M dwarfs, then the overall occurrence rate must be lower by a factor of 3–10 than that for FGK dwarfs.

Subgiant stars—those stars that have exhausted their core hydrogen and swollen in size by a factor of a few—present an interesting puzzle. Compared with main-sequence stars, subgiants are deficient in short-period giant planets ( $P \lesssim 0.3$  year) and over-endowed with longer-period giant planets ( $\gtrsim 3$  year), and their planets tend to have lower eccentricities (Johnson et al. 2010). These differences may be connected to the larger masses of the subgiants that were surveyed; indeed, the surveys were designed to investigate 1.2–2.5  $M_{\odot}$

stars, which are not amenable to precise Doppler observations when they are on the main sequence (Johnson et al. 2006). However, there is now evidence, based on analyses of selection effects (Lloyd 2011) and kinematics (Schlaufman & Winn 2013), that the subgiants are not as massive as previously thought. Possibly, the differences in planet populations are attributable to stellar age or size rather than mass, although none of the proposed scenarios can account for all the observations. For example, the deficit of close-in planets may be caused by the subgiants’ enhanced rate of tidal dissipation, which makes close-in planets vulnerable to orbit shrinkage and engulfment (Villaver & Livio 2009, Schlaufman & Winn 2013), but this would not explain the over-abundance of giant planets in wider orbits.

## 2.2 Transiting planets

Selection effects are severe for transit surveys. In addition to the obvious requirement that the planetary orbit be oriented nearly perpendicular to the sky plane, there are strong biases favoring large planets in tight orbits. In an idealized wide-field imaging survey, the effective number of stars that can be searched for transits varies as the orbital distance to the  $5/2$  power and the planet radius to the sixth power (Pepper et al. 2003). It is a struggle to bring the occurrence rate to light when buried beneath such heavy biases.

The best opportunity to do so was provided by the *Kepler* space telescope, which monitored  $\approx 150,000$  FGKM dwarfs for four years and was uniquely sensitive to planets as small as Earth with periods approaching one year. Ideally, occurrence rates would be based on an analysis accounting for (a) the possibility that many transit-like signals are actually eclipsing binaries, (b) the efficiency of the transit-searching algorithm, (c) the uncertainties and selection effects in the stellar parameters, and (d) the fact that many target stars are actually multiple-star systems. No published study has all these qualities. Significant steps toward this ideal were made by Fressin et al. (2013), who estimated the number of eclipsing binaries that are intermingled with the planetary signals, and Petigura et al. (2013), who quantified the sensitivity of their searching algorithm.

The flat distribution of planet occurrence in  $\log P$ , and the relative deficit of planets inward of  $P \lesssim 10$  days, were seen initially by Howard et al. (2012) and supported by other studies, including those cited above as well as by Youdin (2011), Dong & Zhu (2013), and Silburt et al. (2014). At the very shortest periods ( $P < 1$  day) is a population of “lava worlds” smaller than  $2 R_{\oplus}$ , which are approximately as common as hot Jupiters (Sanchis-Ojeda et al. 2014).

Several groups have investigated how occurrence rates depend on the host star’s spectral type. Howard et al. (2012) and Mulders et al. (2014) found small planets to be more abundant around smaller stars (unlike giant planets; see § 2.1). This finding was also supported by Dressing & Charbonneau (2013), who focused exclusively on M dwarfs because they offer the potential to detect the smallest planets.

One seemingly straightforward test is to compare the transit and Doppler results for the occurrence rate of hot Jupiters, because those planets are readily detected by both methods. The transit surveys give a significantly lower rate (see Table 1), testifying to the difficulty of accounting for selection effects. The discrepancy might be attributable to differences in age, metallicity, or the frequency of multiple-star systems between the two samples (Gould et al. 2006, Bayliss & Sackett 2011, Wright et al. 2012).

Another interesting property of hot Jupiter hosts, seen in both Doppler and transit data, is their tendency to have fewer planets with periods between 10-100 days than stars without hot Jupiters. Wright et al. (2009) used Doppler data to show that systems with more than

one detected giant planet rarely include a hot Jupiter, and Steffen et al. (2012) used *Kepler* data to show that hot Jupiters are less likely than longer-period giants to show evidence for somewhat more distant planetary companions.

### 2.3 Microlensing planets

Microlensing surveys are more sensitive to distant planets than Doppler and transit surveys. The sweet spot for planetary microlensing is an orbital distance of a few astronomical units, a scale set by the Einstein ring radius of a typical lensing star. Microlensing is especially useful for probing M dwarfs, which are numerous enough to provide most of the optical depth for lensing. Microlensing is also capable of detecting planets that roam the galaxy untethered to any star (Sumi et al. 2011). Against these strengths must be weighed the relatively small number of detected planetary events, the poor knowledge of the host star’s properties, and the difficulty of follow-up observations to confirm or refine the planetary interpretation.

Gould et al. (2010) analyzed a sample of 13 microlensing events that led to six planet discoveries, allowing a measurement of the frequency of planets with planet-to-star mass ratios  $q \sim 10^{-4}$  (probably Neptune-mass planets around M dwarfs) and sky-projected orbital separations  $s \sim 3$  AU. They expressed the result as

$$\frac{dN}{d \log q d \log s} = 0.36 \pm 0.15 \quad (2)$$

This study, as well as those by Sumi et al. (2011) and Cassan et al. (2012), found that Neptune-mass planets are common around M dwarfs; indeed, they are just as common as one would predict by extrapolating Equation (1). This sounds like good agreement until it is recalled that Equation (1) was based on Doppler surveys of FGK dwarfs and that those same surveys found giant planets ( $\gtrsim 0.3 M_{\text{Jup}}$ ) to be rarer around M dwarfs. The combination of Doppler and microlensing surveys thereby suggests that M dwarfs have few Jovian planets but a wealth of sub-Jovian planets at orbital distances  $\gtrsim 1$  AU (Clanton & Gaudi 2014).

### 2.4 Directly imaged planets

The technological challenges associated with direct imaging have limited the results to the outer regions of relatively young and nearby stars. Young stars are preferred because young planets are expected to be more luminous than older planets. In addition, direct imaging is based on detection of planet luminosity, which must be related to planet mass or size through uncertain theoretical models. Some stunning individual systems have been reported (Marois et al. 2010, Lagrange et al. 2010), but the surveys indicate that fewer planets are found than would be predicted by extrapolating the power-law of Equation (1) out to 10-100 AU (Lafrenière et al. 2007, Nielsen & Close 2010, Biller et al. 2013, Brandt et al. 2014).

### 2.5 Earth-like planets

How common are planets that are similar to the Earth? Until a few years ago the main obstacle to an answer was the absence of data. Now that the Doppler surveys and the *Kepler* mission have taken us to the threshold of detecting Earth-like planets, the main obstacle is turning the question into a well-posed calculation.



Table 2. Occurrence rates of “Earth-like planets”

Type of star	Type of planet	Approx. HZ boundaries* [ $S/S_{\oplus}$ ]	Occurrence rate [%]	Reference
M	1-10 $M_{\oplus}$	0.75-2.0	$41^{+54}_{-13}$	1
FGK	0.8-2.0 $R_{\oplus}$	0.3-1.8	$2.8^{+1.9}_{-0.9}$	2
FGK	0.5-2.0 $R_{\oplus}$	0.8-1.8	$34 \pm 14$	3
M	0.5-1.4 $R_{\oplus}$	0.46-1.0	$15^{+13}_{-6}$	4
M	0.5-1.4 $R_{\oplus}$	0.22-0.80	$48^{+12}_{-24}$	5
GK	1-2 $R_{\oplus}$	0.25-4	$22 \pm 4$	6
FGK	1-2 $R_{\oplus}$	$\sim 0.9$ -2.2 <sup>†</sup>	$\sim 0.01^{\dagger}$	7
FGK	1-4 $R_{\oplus}$	0.35-1.0	$6.4^{+3.4}_{-1.1}$	8
G	0.6-1.7 $R_{\oplus}$	0.51-1.95	$1.7^{+1.8}_{-0.9}$	9

Note. — References: (1) Bonfils et al. (2013), (2) Catanzarite & Shao (2011), (3) Traub (2012), (4) Dressing & Charbonneau (2013), (5) Kopparapu (2013), (6) Petigura et al. (2013), (7) Schlaufman (2014), (8) Silburt et al. (2014), (9) Foreman-Mackey et al. (2014). In column 3,  $S$  refers to the incident flux of starlight on the planet, and  $S_{\oplus}$  to the Earth’s insolation. All these works are based on *Kepler* data except (1) which is based on the HARPS Doppler survey, and (7) which is based on both *Kepler* and the Keck Doppler survey. \*In many cases the actual HZ definitions used by the authors were more complex; please refer to the original papers for details. <sup>†</sup>The result is much lower than the others because the author also required the Earth-sized planet to have a long-period giant-planet companion.

The criteria for being Earth-like are usually taken to be a range of sizes or masses bracketing the Earth, and a range of values for the incident flux of starlight  $S = L_{\star}/4\pi a^2$ , in which  $L_{\star}$  is the stellar luminosity and  $a$  is the orbital distance. The range of  $S$  is chosen so that the planet is placed in the habitable zone, in which liquid water would be stable on the surface of an Earth-like planet (Kasting et al. 1993, Seager 2013, Guedel et al. 2014). The  $S$ -range may depend on the type of star; this conclusion is based on models that account for the stellar spectrum and its interaction with the presumed constituents of the planet’s atmosphere. Table 2 summarizes the recent estimates.

Much could be written about the virtues and defects of these studies and why they disagree. It is probably more useful to make a broader point. The occurrence rate is an integral of a probability density over a chosen range of parameters, and in this case the uncertainty is limited for the foreseeable future by our ignorance of the appropriate limits of integration. For example, Petigura et al. (2013) reported results differing by a factor of nine depending on the definition of the habitable zone. Likewise, Dressing & Charbonneau (2013) and Kopparapu (2013) used the same probability density to derive occurrence rates differing by a factor of three.

In addition there may be other crucial aspects of habitability beyond size and insolation. Must a planet’s atmosphere be similar to that of the Earth (Zsom et al. 2013)? Must the planet enjoy the white light of a G star, as opposed to the infrared glow of an M dwarf (Tarter et al. 2007)? For now, the best approach is probably to report the probability density near Earth-like parameters (Foreman-Mackey et al. 2014) and allow astrobiologists

the freedom of interpretation.

### 3 ORBITAL DISTANCE AND ECCENTRICITY

Planets in the Solar System have orbital distances between 0.3 and 30 AU, a much narrower range than is allowed from basic physical considerations. For the minimum distance, a planet must be outside the Roche limit ( $a \gtrsim 0.01$  AU), the distance within which the star’s tidal force prevents a planet from maintaining hydrostatic equilibrium. The Roche limit can be stated conveniently in terms of the orbital period and planetary mean density (Rappaport et al. 2013) and corresponds to  $P \gtrsim 12$  hours for a gas giant and  $\gtrsim 5$  hours for a rocky planet. As for the maximum distance, stable orbits are limited to  $a \lesssim 10^5$  AU by perturbations from random encounters with other stars as well as the overall Galactic tidal field (Heisler & Tremaine 1986, Veras et al. 2009).

Regarding orbital shapes, in Newtonian gravity the eccentricity  $e$  may range from 0 to 1, and the orbital energy is independent of eccentricity for a given semimajor axis. This is why the nearly circular orbits in the Solar System seem to require a special explanation, involving either the initial conditions of planet formation or processes that tend to circularize orbits over time.

#### 3.1 Doppler planets

Most of our knowledge of eccentricities comes from the Doppler technique. Many orbits are consistent with being circular; for some of the closest-in planets the eccentricities have upper bounds on the order of  $\sim 10^{-3}$ . On the other side of the distribution are giant planets with eccentricities of 0.8–0.9. Among the systems with very secure measurements, the most eccentric orbit belongs to HD 80606b ( $e = 0.93$ ; Naef et al. 2001, Hébrard et al. 2010).

The left panel of Figure 3 shows the observed eccentricity–period distribution. No correction was made for selection effects; the apparent excess of planets with periods of a few days is the result of the strong bias favoring the detection of short-period giant planets. The data points have been given colors and shapes to convey the metallicity of the host star, and whether or not additional planets have been detected, for reasons to be described. For comparison, the right panel of Figure 3 shows the  $e$ – $P$  distribution of the same number of eclipsing binary stars, which have been drawn randomly from the SB9 catalog (Pourbaix et al. 2004).

At a glance, the planetary and stellar distributions are similar: both have preferences for circular orbits at the shortest periods, and eccentricity distributions that broaden with increasing period. The dashed lines are approximately where the closest approach between the two bodies is 0.03 AU ( $6.5 R_{\odot}$ ), which seems to set an upper limit for the eccentricity as a function of period in both cases. The likely explanation for this eccentricity envelope is tidal dissipation. Time-varying tidal forces lead to periodic distortions and fluid flows on both bodies. The inevitable friction associated with those motions gradually dissipates energy, one consequence of which is the circularization of the orbit (see, e.g., Ogilvie 2014).

For planets, the eccentricity distribution is often modeled with a Rayleigh function,

$$\frac{dN}{de} = \frac{e}{\sigma^2} \exp\left(-\frac{e^2}{2\sigma^2}\right), \quad (3)$$

motivated in part by Jurić & Tremaine (2008), who found this to be the expected long-term outcome of planet–planet interactions in closely-spaced multiplanet systems. However, a

Rayleigh distribution only fits the high-eccentricity portion of the observed distribution.

Shen & Turner (2008) proposed a different fitting function,

$$\frac{dN}{de} \propto \frac{1}{(1+e)^a} - \frac{e}{2^a}, \quad (4)$$

which gives a good single-parameter description of the data with  $a = 4$  (the purple curve in Fig. 3). Wang & Ford (2011) considered this model as well as more complex functions, such as a combination of a Rayleigh function (which fits the high- $e$  end) and an exponential function (for the more circular systems), finding that the sample sizes were insufficient to make distinctions between these various models. Hogg et al. (2010) and Kipping (2013) advocated the two-parameter beta distribution,

$$\frac{dN}{de} = \frac{\Gamma(a+b)}{\Gamma(a)\Gamma(b)} e^{a-1}(1-e)^{b-1}, \quad (5)$$

which has a number of desirable mathematical properties and provides a good fit for  $a = 0.867$ ,  $b = 3.03$  (the green curve in Fig. 3).

Some authors have noted differences in the period–eccentricity distributions among various subsamples of planets:

1. Wright et al. (2009) noted that systems for which more than one planet has been detected tend to have lower eccentricities than those for which only a single planet is known. The effect is perhaps best articulated as an absence of the very highest eccentricities from the subsample of multiplanet systems, as can be seen by comparing the circles (singles) and stars (multiples) in Figure 3. It might be explained as a “natural selection” effect: In compact multiplanet systems, low eccentricities are more compatible with long-term dynamical stability. Limbach & Turner (2014) went further to show that among the multiplanet systems, the median eccentricity declines with the number of known planets:  $e_m \propto N^{-1.2}$ .
2. Dawson & Murray-Clay (2013) found that giant planets around metal-rich stars have higher eccentricities than similar planets around metal-poor stars. This is manifested in Figure 3 as a deficiency of blue (metal-poor) points with  $P \approx 10$ -100 days and  $e \gtrsim 0.4$ . Dawson & Murray-Clay (2013) theorized that metal-rich stars had protoplanetary disks that were rich in solid material and consequently formed more planets that could engage in planet-planet interactions and excite eccentricities. Adibekyan et al. (2013) reported another intriguing trend involving metallicity: The orbital periods tend to be longer around metal-poor stars than around metal-rich stars.
3. Smaller planets tend to have lower eccentricities (Wright et al. 2009, Mayor et al. 2011), as seen in Figure 4. Small planets are also more likely than giant planets to be found in multiplanet systems (Latham et al. 2011), reinforcing the association between multiplanet systems and lower eccentricity. An important caveat is that eccentricity is especially difficult to measure when the signal-to-noise ratio is low, as is usually the case for small planets (see, e.g., Shen & Turner 2008, Zakamska et al. 2011). For this and other reasons, Hogg et al. (2010) recommended modeling the eccentricity distribution on the basis of Bayesian analysis of the ensemble of Doppler measurements, rather than on a histogram of “best values” of each system’s eccentricity; however, no such analysis has yet been published.

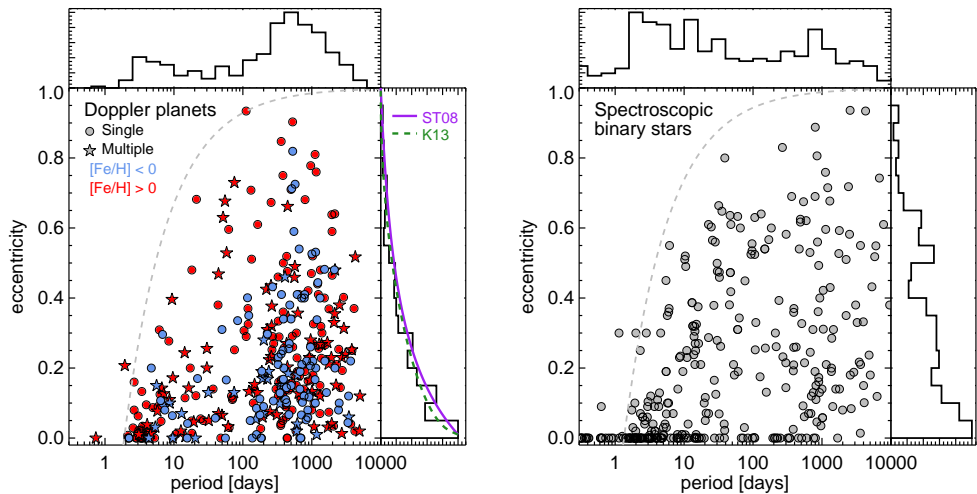


Figure 3 *Left*.—Orbital eccentricity and period for Doppler planets detected with a signal-to-noise ratio  $>10$ , based on an October 2014 query of the `exoplanets.org` database (Wright et al. 2011b). The distribution has not been corrected for selection effects. Red and blue points represent host star metallicities above and below (respectively)  $[\text{Fe}/\text{H}] = 0$ . Stars represent systems in which more than one planet has been detected, whereas circles are single-planet systems. The dashed line shows where the minimum orbital separation would be 0.03 AU for a Sun-like star. The purple curve is Equation (4), taken from Shen & Turner (2008), and the green dashed curve is Equation (5) from Kipping (2013). *Right*.—Eccentricity and period for spectroscopic binary stars from the SB9 catalog (Pourbaix et al. 2004). A random subsample was drawn, to match the number of exoplanet systems. The dashed line shows where the minimum orbital separation would be 0.03 AU for a pair of Sun-like stars. In the marginalized eccentricity distribution, the very large number of systems consistent with  $e = 0$  is not shown.

### 3.2 Transiting planets

Most of the known planets smaller than Neptune were discovered by the *Kepler* mission using the transit technique, which does not directly reveal the orbital eccentricity. The usual way to measure the eccentricity of a transiting planet is to undertake Doppler observations, but for *Kepler* systems this has proven impractical because the stars are too faint. Even in those few cases in which Doppler observations have been performed, the signal-to-noise ratio is too low for secure eccentricity measurement (Marcy et al. 2014). Nevertheless, enticed by the prospect of unveiling the eccentricity distribution for small planets, investigators have pursued other approaches.

**3.2.1 TRANSIT DURATIONS** The transit duration is approximately

$$T = \left( \frac{R_* P}{\pi a} \sqrt{1 - b^2} \right) \frac{\sqrt{1 - e^2}}{1 + e \sin \omega}, \quad (6)$$

where  $\omega$  is the argument of pericenter and  $b$  is the impact parameter, the minimum sky-plane distance between the star and planet expressed in units of the stellar radius  $R_*$ . If the factor

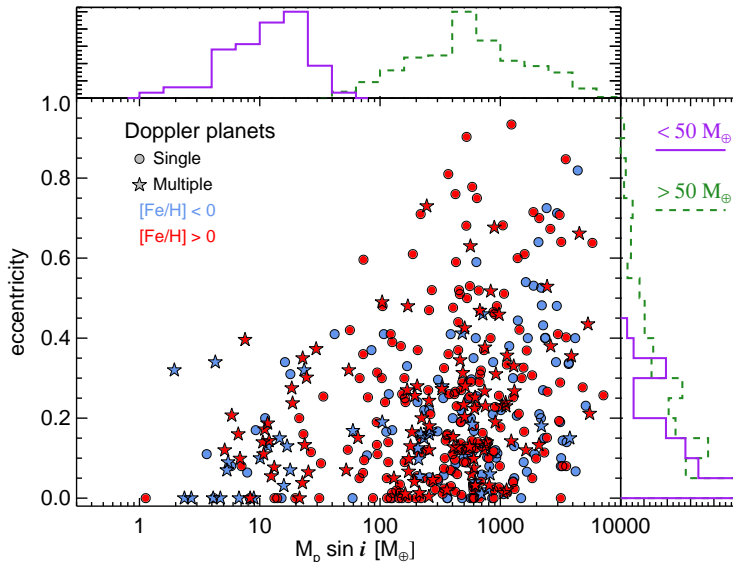


Figure 4 Minimum mass ( $M_p \sin i$ ) and eccentricity of planets detected by the Doppler method with a signal-to-noise ratio  $\geq 5$ , based on an October 2014 query of the `exoplanets.org` database (Wright et al. 2011b). The distribution is *not* corrected for selection effects. Colors and symbol shapes follow the same conventions as in Fig. 3. In the marginalized histograms of period and  $M_p \sin i$ , the blue curve is for planets with  $M_p \sin i < 50 M_\oplus$  and the orange curve is for planets with  $M_p \sin i > 50 M_\oplus$ .

in parentheses is known, then measuring  $T$  provides some eccentricity information. This type of analysis can be performed for an individual transiting planet (Dawson & Johnson 2012), a system of multiple transiting planets (Kipping et al. 2012) or an ensemble of different stars with transiting planets (Ford et al. 2008, Burke 2008).

Moorhead et al. (2011) applied this method early in the *Kepler* mission and found tentative evidence that smaller planets tend to have lower eccentricities than giant planets, and that systems of multiple transiting planets have lower eccentricities than those for which only a single transiting planet was known. Kane et al. (2012) and Plavchan et al. (2014) attempted to improve upon this analysis by taking advantage of several years of additional *Kepler* data, but the results are limited by systematic uncertainties in the stellar properties rather than data volume. Sliski & Kipping (2014) examined the small subset ( $\approx 100$ ) of planet-hosting stars that are especially well characterized, due to the detection of asteroseismic oscillations, and found that the eccentricity distribution could not be distinguished from that of the Doppler sample.

**3.2.2 DYNAMICAL MODELING** In multiplanet systems, the non-Keplerian effects of planet-planet interactions cause perturbations in the transit times and durations that depend on the planets’ masses and orbital elements (Holman & Murray 2005, Agol et al. 2005). With enough data, those parameters may be determined or bounded. This method works best when all the relevant planets are transiting; otherwise the solutions are not

unique (see, e.g., Ballard et al. 2011, Veras et al. 2011).

Applications of this method have confirmed that the eccentricities are low in compact multiplanet systems. For example, Lissauer et al. (2013) showed that at least five of the six known planets in the Kepler-11 system have eccentricities  $< 0.1$ , with the best-constrained planet having  $e < 0.02$ . Similar results were obtained for the Kepler-30 and Kepler-36 systems (Sanchis-Ojeda et al. 2012, Carter et al. 2012). It is not clear, though, whether the systems that were selected for these intensive studies are representative of small-planet systems.

Lithwick et al. (2012) made an important advance enabling the study of a larger sample of small planets. They devised an analytic theory for the transit-timing variations of pairs of planets near a first-order mean-motion resonance (e.g., a period ratio of 2:1 or 3:2). In such a situation, seen in dozens of *Kepler* systems, the sequence of timing anomalies is a nearly sinusoidal function of time. The amplitude and phase of this function depend on a combination of the planet masses and eccentricities. In general the mass and eccentricity of a given planet cannot be determined uniquely, but the method can be used to constrain the eccentricity distribution of a population. Wu & Lithwick (2013) applied this method to 22 pairs of small planets. They found that 16 pairs are consistent with very low eccentricities; the best-fitting Rayleigh distribution had a mean eccentricity of 0.009. The other 6 pairs have higher eccentricities, probably in the range of 0.1–0.4.

## 4 MULTIPLANET SYSTEMS

### 4.1 Multiplicity

We do not know the average number of planets orbiting a given star; this is due to the incompleteness of the detection techniques. However, every technique that has successfully found single planets has also provided at least one case of a multiplanet system. The first known multiplanet system, PSR 1257+12, was shown to have multiple planets on the basis of time delays in the arrival of radio pulses from the central pulsar caused by the pulsar’s orbital motion (Wolszczan & Frail 1992). The data were precise enough to reveal non-Keplerian effects that were due to planet-planet interactions, allowing Konacki & Wolszczan (2003) to derive orbital eccentricities, inclinations, and true masses (as opposed to  $M_p \sin i$ ) for two of the three known planets. This gave a preview of the type of architectural information that would only become available a decade later for planets around normal stars.

Microlensing surveys have found two different two-planet systems (Gaudi et al. 2008, Han et al. 2013), both of which feature giant planets with orbital distances of a few astronomical units. Direct imaging has delivered a spectacular system of four giant planets that have orbital distances of  $\approx 12$ –70 AU (HR 8799; Marois et al. 2010). Because of the slow orbital motion, only small arcs of the four orbits have been mapped out, preventing complete knowledge of the system’s architecture. The large planet masses and closely spaced orbits have prompted theorists to suggest that long-term dynamical stability is possible only if the planets are in particular resonances (Fabrycky & Murray-Clay 2010, Goździewski & Migaszewski 2014).

Until recently, the Doppler technique provided the largest cache of multiplanet systems (Wright et al. 2009, Wittenmyer et al. 2009, Mayor et al. 2011). Then the *Kepler* mission vaulted the transit technique to the top position, identifying hundreds of transiting multiplanet systems (Latham et al. 2011, Burke et al. 2014). Both the Doppler and *Kepler* surveys have shown that compact multiplanet systems with  $P \lesssim 1$  year are usually com-

posed of planets smaller than Neptune and that Jovian planets are uncommon (Wright et al. 2009, Latham et al. 2011). Also noteworthy is that many planets in compact systems have very low densities ( $\lesssim 1 \text{ g cm}^{-3}$ ; see, e.g., Lissauer et al. 2013, Wu & Lithwick 2013, Masuda 2014), which have mainly been revealed through the transit-timing method. The prevalence of small, low-density planets could be a clue about their formation. It may also be related to the requirement for long-term stability. When a closely packed system suffers from dynamical instability, massive planets are more likely to eject one another, whereas smaller planets are more likely to collide until the system stabilizes (Ford & Rasio 2008).

## 4.2 Orbital spacings

In the Solar System, the orbital spacings of planets and their satellites are organized around two themes. The first theme is the nearly geometric progression of orbital distances, which is famously encoded in the Titius-Bode “law”:

$$a_n \text{ [AU]} = 0.4 + 0.3 \times 2^n. \quad (7)$$

This charmingly simple formula loses much of its appeal after learning that  $n$  does not simply range over integers, but rather  $n = -\infty, 0, 1, 2, \dots$ ;  $n = 3$  corresponds to the asteroid belt rather than a planet; and the formula fails for Neptune. Whether this formula has any deep significance is a question that has bewitched investigators since the 18th century. However, there is a sound physical reason to expect a constant ratio of orbital spacings, rather than constant differences or a random pattern: the scale-free nature of gravitational dynamics (Hayes & Tremaine 1998).

The second theme is mean-motion resonance, characterized by period ratios that are nearly equal to ratios of small integers. This is seen most clearly in the satellites of the giant planets, most famously the 1:2:4 resonances of the inner Galilean satellites of Jupiter. Roy & Ovenden (1954) used the ensemble of satellite systems known then to show that the period ratios are closer to low-integer ratios than chance alone would produce, and Goldreich & Soter (1966) summarized the arguments that at least some of those configurations represent the outcome of long-term tidal evolution.

Geometric progressions and mean-motion resonances have also been seen in exoplanetary systems. We begin this discussion by inspecting the orbital spacings in the Doppler systems (which mainly involve giant planets) and the *Kepler* systems (which mainly involve smaller planets). Figure 5 shows the period ratios of all planet pairs discovered by the Doppler technique. For planet pairs with a total mass exceeding  $1 M_{\text{Jup}}$ , there is a clustering of points within the 2:1 resonance that is unlikely to be a statistical fluke (Wright et al. 2011c).

The situation is different for lower-mass planets. Figure 6 shows the period ratios of *Kepler* multiplanet systems (Burke et al. 2014). Within this sample, dominated by small planets with periods shorter than a few hundred days, there is only a weak preference for period ratios near resonances (Lissauer et al. 2011). This finding was initially surprising because the Doppler systems had already shown a stronger preference for resonances, and because the theory of disk migration—by which wide-orbiting planets are conveyed to smaller orbits through gravitational interactions with the protoplanetary disk—predicted that planet pairs would often be caught into resonances (Goldreich & Tremaine 1980, Lee & Peale 2002). Retrospectively, it has been possible to find ways to avoid this faulty conclusion (Goldreich & Schlichting 2014, Chatterjee & Ford 2015).

Closer inspection of Figure 6 reveals subtle features: there appears to be a tendency to avoid exact resonances (Veras & Ford 2012), and prefer period ratios slightly larger

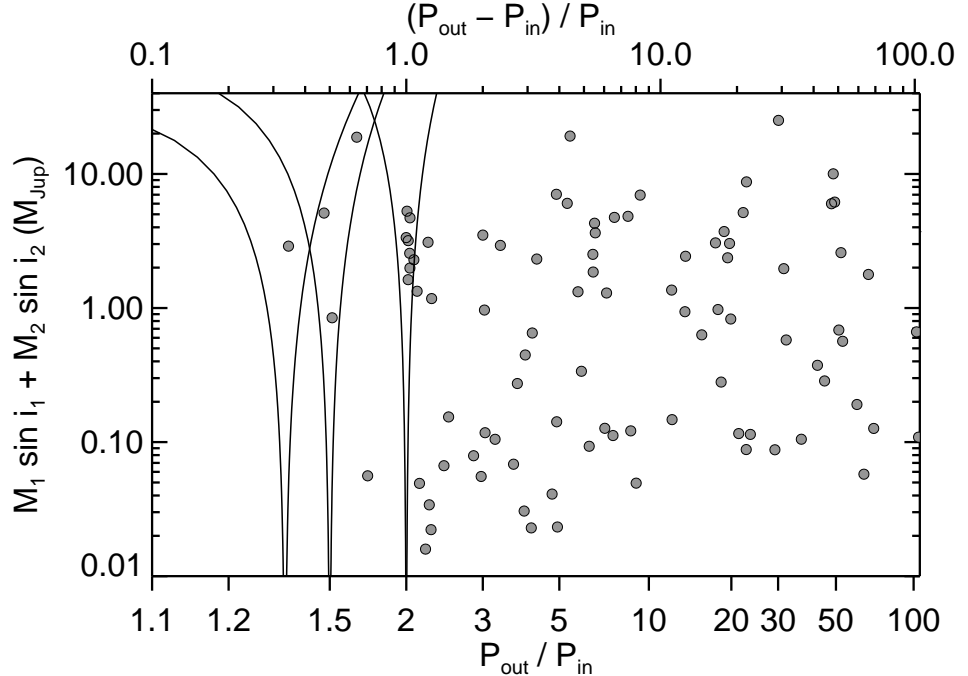


Figure 5 Period ratios of Doppler planet pairs. The horn-shaped curves show the approximate resonance boundaries,  $|P_{\text{out}} - jP_{\text{in}}|/P_{\text{in}} = 0.05((M_1 + M_2)/M_{\text{Jup}})^{1/2}$ , for each  $(j + 1) : j$  resonance. Pairs with larger planet masses are more often found in resonances. Based on an August 2014 query of [exoplanets.org](http://exoplanets.org) (Wright et al. 2011b).

than the resonant values (Fabrycky et al. 2014). Specifically, there is a deficit of pairs with period ratios of 1.99–2.00 and an excess of pairs with period ratios of 1.51 and 2.02. This finding was anticipated by Terquem & Papaloizou (2007) as a consequence of tidal dissipation within the inner planet that would cause the orbits to spread apart, an idea that was picked up again by Batygin & Morbidelli (2013) and Lithwick, Xie & Wu (2012) once the *Kepler* sample became available.

Despite this interest in the nearly-resonant systems, the main lesson of Figure 6 is that resonances are uncommon among small planets with periods shorter than a few years. The most commonly observed period ratios are in the range of 1.5–3.0, a good match to the period ratios of the Solar System (1.7–2.8). The smallest confirmed period ratio of 1.17 belongs to Kepler-36. That system features two unusually closely spaced planets with densities differing by a factor of 8 and transit times exhibiting large and erratic variations (Carter et al. 2012). The fits to the data suggest the planets’ orbits are chaotic, with a Lyapunov time of approximately 20 years, and yet they manage to remain stable over long timescales (Deck et al. 2012).

One way in which the periods in the Solar System differ from a purely geometric progression is that the period ratio tends to be larger for the more distant planets; this is encoded in Equation (7) by the constant term of +0.4. This progressive widening of period ratios has not been seen in exoplanetary systems. In fact Steffen & Farr (2013) found an opposite trend: The period ratios tend to be larger for the very closest planets. This can be



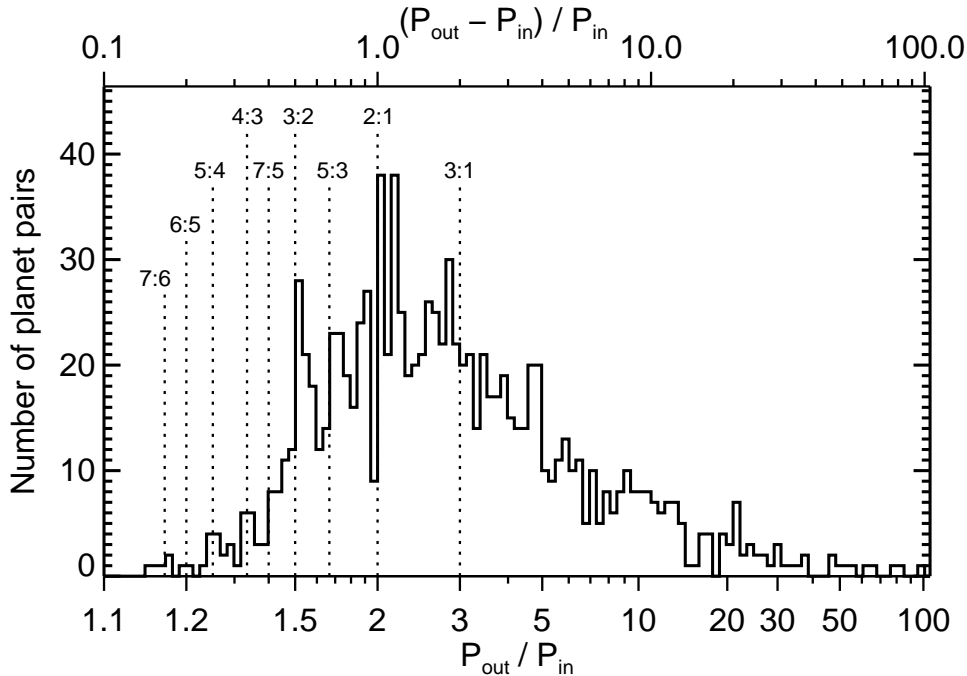


Figure 6 Period ratios of *Kepler* planet pairs, based on the sample by Burke et al. (2014). The top axis indicates the fractional period difference, and the histogram bin widths represent  $1/40$  of the logarithm of this quantity. The bottom axis indicates the period ratio.

seen in Figure 7, which displays the periods of the *Kepler* multiplanet systems. For those systems with an innermost planet at  $P < 3$  days, the period ratio between the innermost two planets is larger than that of other systems. Perhaps the innermost planets are being pulled closer to the star by tidal dissipation (Teitler & Königl 2014, Mardling 2007).

### 4.3 Mutual inclination

The coplanarity of the Solar System is compelling evidence that the planets originated within a flat rotating disk. The underlying logic is that the laws of dynamics allow for higher mutual inclinations; the current Solar System does not have any mechanism for damping inclinations; therefore, the low inclinations must be attributed to the initial conditions.

This is probably correct, although the argument is not watertight because large mutual inclinations tend to make systems more vulnerable to dynamical instability. For example, in the Kozai-Lidov instability, mutual inclinations excite eccentricities and eventually cause the orbits to intersect. This raises the possibility that highly inclined systems are created in abundance but tend to destroy themselves. Veras & Armitage (2004) derived inclination-dependent formulas for the minimum separation between planetary orbits compatible with long-term stability. They predict that even small mutual inclinations are potentially lethal to closely packed systems of small planets. For example, the minimum spacing between two  $3 M_{\oplus}$  planets around a Sun-like star is twice as large for  $\Delta i = 5^{\circ}$  as it is for coplanar orbits.

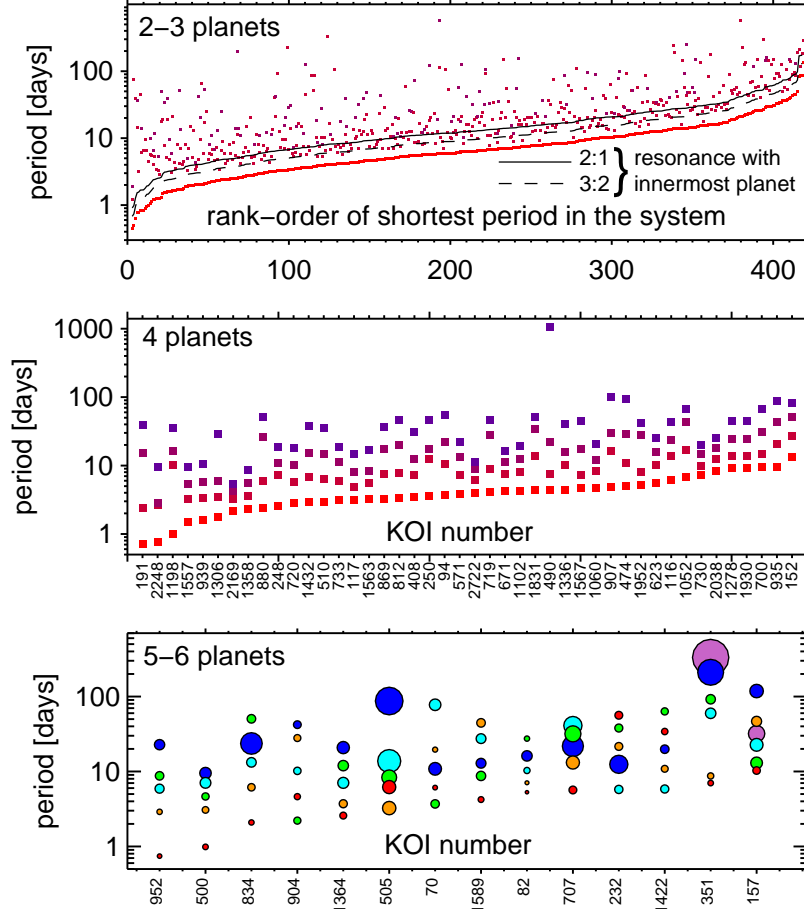


Figure 7 Multitransiting planetary systems from *Kepler*. Each symbol represents one planet. All the symbols along a given vertical line belong to the same star. The systems are ordered horizontally according to the innermost planet’s orbital period. *Top.*—Systems with two or three detected transiting planets ( $N_{\text{tra}} = 2-3$ ). *Middle.*—Systems with  $N_{\text{tra}} = 4$ . *Bottom.*—Systems with  $N_{\text{tra}} = 5-6$  planets. The symbol size is proportional to planetary radius.

There are a few systems for which investigators have used the requirement of long-term stability to place bounds on mutual inclinations. For 47 Uma, Laughlin, Chambers & Fischer (2002) showed that the orbits of the two giant planets are likely to be inclined by less than  $40^\circ$ . Likewise, Nelson et al. (2014) found the orbit of the innermost planet of 55 Cnc to be inclined by  $\lesssim 40^\circ$  from the outer planets (which were assumed to be coplanar).

Directly measuring mutual inclinations is challenging. The astrometric technique could reveal mutual inclinations, but it has proven difficult to achieve the necessary precision. Likewise, direct imaging can do the job, but the only directly imaged multiplanet system (HR 8799) has not been observed for long enough. The Doppler technique is sensitive

to all the planets in a multiplanet system but is generally blind to mutual inclinations. The transit technique would likely miss many planets in a noncoplanar system, and even when multiple transiting planets are seen, they could be mutually inclined with nonparallel trajectories across the stellar disk. Nevertheless, investigators have managed to learn about mutual inclinations by exploiting loopholes in these statements, combining the results of different techniques, and considering population statistics, as we shall now discuss.

**4.3.1 INDIVIDUAL SYSTEMS** Although Doppler data do not ordinarily reveal mutual inclinations, there are a few cases in which the planet-planet interactions produce detectable perturbations in the host star’s motion beyond the simple superposition of Keplerian orbits. In one system, GJ 876, these perturbations are large enough to have allowed the usual fitting degeneracies to be broken and the mutual inclination to be determined. In this system there are two giant planets in a 2:1 resonance along with a smaller inner planet and a Neptune-mass outer planet. The data set is rich enough to have attracted many investigators (Rivera & Lissauer 2001, Ji et al. 2002, Bean & Seifahrt 2009, Correia et al. 2010, Rivera et al. 2010, Baluev 2011) who all concluded that the mutual inclination between the two giants is  $\lesssim 5^\circ$ .

Planet-planet perturbations have been detected in a few other systems, but the Doppler data have too short a timespan to pin down the mutual inclination. One example is the two-planet system HD 82493, for which the data do not specify the mutual inclination, although they do specify the sky-plane inclination of both orbits if they are assumed to be coplanar (Tan et al. 2013). What makes this interesting is that the morphology of the star’s directly imaged debris disk suggests that it has the same inclination as the planetary orbits to within  $4^\circ$  (Kennedy et al. 2013). A second system in which the planet-disk inclination was measured is  $\beta$  Pic. Both the planetary orbit and the disk orientation have been measured through direct imaging, and the planet is aligned with the inner portion of the disk to within a few degrees (Lagrange et al. 2012, Nielsen et al. 2014, Macintosh et al. 2014). The planet-disk alignment seen in these two systems suggests that the systems are relatively flat.

Another special case is the three-planet system  $\Upsilon$  And, for which McArthur et al. (2010) used a combination of Doppler and astrometric data to show that the orbits of the two most massive planets are mutually inclined by  $30 \pm 1^\circ$ . This remains the only direct demonstration of a mutual inclination greater than a few degrees and is therefore an important result that deserves to be checked against additional data. Earlier, the same technique gave an inclination near  $90^\circ$  for one of the GJ 876 planets (Benedict et al. 2002), but this result was cast into doubt after being found inconsistent with the seemingly more reliable results of the Doppler analysis (Bean & Seifahrt 2009).

The four-planet system Kepler-89 was kind enough to schedule a planet-planet eclipse during the *Kepler* mission, when one planet eclipsed another planet while both were transiting the star. Hirano et al. (2012) used the timing and duration of this extraordinary event to show that the angle between the two orbits was smaller than a few degrees. The next such eclipse in Kepler-89 is not expected until 2026, and no planet-planet eclipses have been identified for any other system, apart from one problematic candidate (Masuda 2014).

Finally, a potentially powerful method to determine mutual inclinations is the analysis of variations in transit times and durations, as described earlier in the context of orbital eccentricities (§ 3.2.2). For instance, the Kepler-30 system features three transiting giant planets, and the observed absence of transit duration variations requires that the mutual inclinations be smaller than a few degrees (Sanchis-Ojeda et al. 2012). Dynamical modeling

has also been used to limit mutual inclinations to  $\lesssim 10^\circ$  in the multitransiting systems Kepler-9 (Holman et al. 2010), Kepler-11 (Lissauer et al. 2011), Kepler-36 (Carter et al. 2012) and Kepler-56 (Huber et al. 2013). These results are all consistent with coplanarity, but one is left wondering whether this is a selection effect because of the requirement that all the planets transit the host star. Addressing this concern, Nesvorný et al. (2012) analyzed the Kepler-46 system, in which there is only one transiting planet but it exhibits unusually large transit-timing variations, allowing the inference of a nontransiting outer planet with an orbit that is aligned with the transiting planet to within about  $5^\circ$ . Similar results, although with coarser accuracy, have been obtained for several other systems (Nesvorný et al. 2013, 2014; Dawson et al. 2014).

**4.3.2 POPULATION ANALYSIS** Apart from the individual cases described above, statistical arguments have been used to investigate the typical mutual inclinations of multiplanet systems, thanks to the large number of such systems that the Doppler and *Kepler* surveys have provided. Dawson & Chiang (2014) provided indirect evidence for large mutual inclinations in five giant-planet systems. Their argument was based on the inference that the major axes of the two orbits are more nearly perpendicular than would have occurred by chance. This preference for perpendicularity is predicted in a model for the origin of giant planets with eccentric orbits and  $a = 0.1\text{--}1$  AU. In this model, the planets' orbits are inclined by  $35\text{--}65^\circ$  and perturb each other gravitationally, ultimately causing the inner planet's orbit to shrink as a result of eccentricity cycling and intermittent tidal dissipation (see also Dong et al. 2014).

All the other statistical investigations of mutual inclination have concentrated on the compact systems of multiple planets rather than on giant planets:

1. One approach is to analyze the transit multiplicity distribution, defined as the relative occurrence of systems with differing numbers of transiting planets. All other things being equal, systems of higher transit multiplicity are more likely to be detected if the mutual inclinations are low. Tremaine & Dong (2012) presented a general formalism for assessing the agreement between planet models with differing degrees of coplanarity and the observed number of transiting systems of different multiplicities. They concluded that, with only the transit data, mutual inclinations are not well-constrained because of a degeneracy with the typical number of planets per star: With more planets per star, one can reproduce the *Kepler* statistics with larger mutual inclinations. A similar conclusion was reached by Lissauer et al. (2011).
2. Lissauer et al. (2011) noted a potentially interesting pattern in the multiplicity distribution. When modeling the mutual inclination distribution as a Rayleigh function, they had difficulty fitting the large observed ratio of single-transiting systems to multiple-transiting systems. Their interpretation was that the single-transiting systems are divided into two groups with different architectures. Some are flat systems for which only the inner planet happens to transit; the others are systems with fewer planets or higher mutual inclinations. Several other studies reached the same conclusion (Johansen et al. 2012, Hansen & Murray 2013, Ballard & Johnson 2014). However, Tremaine & Dong (2012) found no such evidence for two separate populations. This may be because they used a more general model for the multiplicity distribution, allowing the fractions of systems with differing numbers of planets to be independent parameters, rather than requiring all stars to have a certain number of planets. Xie et al. (2014) found supporting evidence, based on the relative occurrence

of detectable transit-timing variations, that the single-transiting and multitransiting systems are qualitatively different.

3. A different method, also based on *Kepler* data, employs the transit durations of different planets orbiting the same star. The transit duration varies as  $\sqrt{1 - b^2}$ , in which  $b$  is the impact parameter (defined in § 3.2.1). In a perfectly flat system, more distant transiting planets should have larger impact parameters. This trend should not be present if the typical mutual inclinations are greater than  $R_*/a$ . Therefore, by searching for this trend, one can check for near-coplanarity. Fabrycky et al. (2014) found such a trend among the *Kepler* multiplanet systems and concluded the mutual inclinations are typically smaller than a few degrees. Fang & Margot (2012) combined this technique with multiplicity statistics and came to a similar conclusion.
4. Another method is to combine the results of the Doppler and *Kepler* surveys. If mutual inclinations are typically larger than  $R_*/a$ , then transit surveys would miss many planets in each system, but Doppler surveys would potentially detect them all. A constraint on the typical mutual inclination can therefore be obtained by requiring consistency among the occurrence rates of multiplanet systems seen in Doppler and transit surveys. Among the complications are the differences in the selection effects and stellar populations between the surveys and the need to measure or assume a planetary mass-radius relationship (because Doppler surveys measure mass while transit surveys measure radius). Figueira et al. (2012) performed such a study and concluded the compact systems of small planets ( $\lesssim 2 R_\oplus$ ,  $\lesssim 10 M_\oplus$ ) have typical mutual inclinations smaller than a few degrees (see also Tremaine & Dong 2012).

Taken together these studies paint a picture in which the systems of small planets with periods less than approximately one year—which exist around nearly half of all Sun-like stars—are essentially as flat as the Solar System. The power of these statistical methods has put us in the surprising situation of knowing more about the mutual inclinations of small-planet systems than about giant-planet systems, because giant planets (despite being easier to study in almost every other way) are rarely found in compact multiplanet systems.

## 5 STELLAR ROTATION

By the early 17th century it was known that the Sun rotates with a period of approximately 25 days. This discovery invited comparisons between the Sun’s rotational angular momentum and the planets’ orbital angular momentum. The Sun’s angular momentum is 3.4 times larger than that of the four inner planets, and 185 times smaller than that of the four outer planets. The solar obliquity—the angle between the Sun’s angular momentum vector and that of all the planets combined—is only  $6^\circ$ .

To our predecessors, the low obliquity did not seem remarkable because it harmonized with the low mutual inclinations between the planetary orbits and supported the idea that the Sun and planets inherited their angular momentum from a rotating disk. In contrast, they regarded the Sun’s relatively slow rotation as a dissonance that needed to be explained by the theory of planet formation. For example, the demise of tidal theories of planet formation was partly on account of the difficulty in drawing material from the Sun and endowing it with enough angular momentum to become the outer planets.

In the modern exoplanet literature, the roles of rotation rate and obliquity and have been reversed. Explaining the magnitude of a star’s angular momentum is now recognized as an issue for star-formation theory and subsequent magnetic braking, as opposed to being

directly related to planet formation. However, stellar obliquity has become an active subfield of exoplanetary science, with surprising observations and creative theories.

### 5.1 Stellar rotation rate

Despite this role reversal, a few investigators have searched for relationships between stellar rotation and planetary orbital motion. Rotation rates can be estimated from the rotational contribution to spectral line broadening ( $v \sin i$ , where  $i$  is the inclination angle between the stellar rotation axis and the line of sight) or from the period of photometric modulations caused by rotating starspots. The results show that any rotational differences between planet-hosting stars and similar stars without known planets are modest (Barnes 2001, Alves et al. 2010, Gonzalez 2011, Brown 2014).

The only clear differences pertain to systems with the shortest-period planets, as one may have expected, because such planets are most sensitive to spin-orbit interactions mediated by tides, magnetic fields, or the innermost portion of the protoplanetary disk. For orbital periods shorter than the stellar rotation period, tidal dissipation gradually shrinks the planet’s orbit and spins up the host star. Eventually this process synchronizes the rotational and orbital periods unless the synchronous state would require the rotational angular momentum to be more than 25% of the total angular momentum, in which case the planet spirals into the star (Counselman 1973, Hut 1980). A few cases are known in which spin-orbit synchronization seems to have been achieved ( $\tau$  Boo, Butler et al. 1997; HD 162020, Udry et al. 2002; Corot-4b, Aigrain et al. 2008). In addition, Pont (2009), Brown et al. (2011), Husnoo et al. (2012), and Poppenhaeger & Wolk (2014) highlighted particular cases in which a planet-hosting star is rotating more rapidly than expected, suggesting that tidal spin-up is underway. McQuillan et al. (2013) used *Kepler* data to show that faster-rotating stars ( $P_{\text{rot}} \lesssim 10$  days) do not host short-period planets ( $P_{\text{orb}} \lesssim 3$  days) as often as do slower-rotating stars. This has been interpreted as a sign that the rapid rotators ingested their close-in planets (Teitler & Königl 2014).

### 5.2 Stellar obliquity

Measurements of stellar obliquity have revealed a wide range of configurations, including stars with lower obliquities than the Sun (e.g., HD 189733; Winn et al. 2006), stars with moderate tilts (e.g., XO-3; Hébrard et al. 2008, Winn et al. 2009, Hirano et al. 2011), stars that are apparently spinning perpendicular to their orbits (e.g., WASP-7; ?) and retrograde systems in which the star revolves in the opposite direction as the planet’s rotation (e.g., WASP-17; Triaud et al. 2010).

Much of this knowledge has been obtained by observing the Rossiter-McLaughlin effect, a time-variable distortion in stellar spectral lines caused by a transiting planet (Queloz et al. 2000). Two limitations of these results should be borne in mind. First, only the sky projection of the obliquity can be measured. A small obliquity must have a small sky projection, but a high obliquity may also have a small sky projection. Second, almost all the existing data are for hot Jupiters, for the practical reason that the effect is most easily measured when transits are deep and frequent.

The top panel of Figure 8 shows the hot Jupiter data along with the two clearest patterns that have emerged. First, stars with relatively cool photospheres ( $\lesssim 6100$  K) have low obliquities, whereas hotter stars show a wider range of obliquities (Schlaufman 2010, Winn et al. 2010, ?, Dawson 2014). Second, the highest-mass planets ( $\gtrsim 3 M_{\text{Jup}}$ ) are

associated with lower obliquities (Hébrard et al. 2011).

Suggestively, the boundary of 6100 K coincides with the long-known “rotational discontinuity” above which stars are observed to rotate significantly faster (Kraft 1967). This is demonstrated in Figure 8 in the plot of  $v \sin i$  versus  $T_{\text{eff}}$ . The rotational discontinuity is thought to arise from the differing internal structures of the stars on either side of the boundary. Cool stars have thick convective envelopes and radiative cores, whereas hot stars generally have radiative interiors with only thin convective envelopes and a small convective core. These internal differences cause cool stars to have stronger magnetic fields and magnetic braking, explaining the rotational discontinuity. In addition, cool stars are thought to be capable of dissipating tidal oscillations more rapidly.

It is therefore natural to try and explain the obliquity patterns as consequences of differing rates of rotation, magnetic braking, and tidal dissipation. Regarding rotation, there seems to be no correlation between obliquity and  $v \sin i$  after controlling for effective temperature. Magnetic braking and tidal dissipation are complex and poorly understood processes, with no simple and generally-accepted metrics that can be computed for all the systems [although Albrecht et al. (2012) and Dawson et al. (2014) made efforts in that direction]. A simple dimensionless ratio that characterizes the ability of the planet to tidally deform the star is  $\epsilon_{\text{tide}} \equiv (M_{\text{p}}/M_{\star})(R_{\star}/a)^3$ , and indeed, there is a suggestive pattern involving this tidal parameter. The lower panel of Figure 8 shows projected obliquity as a function of  $\epsilon_{\text{tide}}$  for all the single-planet systems (not only hot Jupiters). The cool stars have a broad range of obliquities for the weakest tides, and low obliquities for  $\epsilon_{\text{tide}} \gtrsim 4 \times 10^{-7}$ . The hot stars have a broad range of obliquities over essentially the entire range and a possible trend toward low obliquity for  $\epsilon_{\text{tide}} \gtrsim 4 \times 10^{-5}$ . These trends suggest that many of the low obliquities are the consequences of tides, which tend to align systems.

No doubt this story is oversimplified. Among the theorists who have pursued more detailed descriptions are Valsecchi & Rasio (2014), who found that misalignment is correlated with the depth of the outer convective zone as calculated in stellar-evolutionary models; and Dawson (2014), who modeled both tidal dissipation and magnetic braking and concluded that the braking rate was the more important difference between hot and cool stars. Winds rob the star of most of its angular momentum, allowing the planet to realign the rest of it. Furthermore, even if the story is correct, it leaves many questions unanswered. In many tidal theories, realignment is accompanied by withdrawal of angular momentum from the planetary orbit, leading to orbital decay. How, then, can the obliquity be lowered without destroying the planet? Lai (2012) provided one possible solution by giving an example of a more complex tidal theory in which realignment can be much faster than orbital decay.

Another unanswered question is the origin of the high obliquities. Are hot Jupiters formed with a wide range of orbital orientations? An affirmative answer would support theories for hot Jupiter production involving planet-planet scattering (Rasio & Ford 1996, Weidenschilling & Marzari 1996) or Kozai-Lidov oscillations (Mazeh et al. 1997, Fabrycky & Tremaine 2007, Naoz et al. 2011). Alternatively, high stellar obliquities may simply be a common outcome of star formation (Bate et al. 2010, Thies et al. 2011, Fielding et al. 2014). Additional possibilities are magnetic star-disk interactions (Lai et al. 2011), or torques from distant stellar companions (Tremaine 1991, Batygin et al. 2011, Storch et al. 2014). Rogers et al. (2012) proposed that high obliquities originate from stochastic rearrangements of angular momentum within hot stars, mediated by gravity waves; in this scenario, the photosphere is rotating in a different direction from the interior.

Answering these questions would be easier if the domain of the obliquity measurements could be expanded to include other types of planets besides close-in giants. Because the

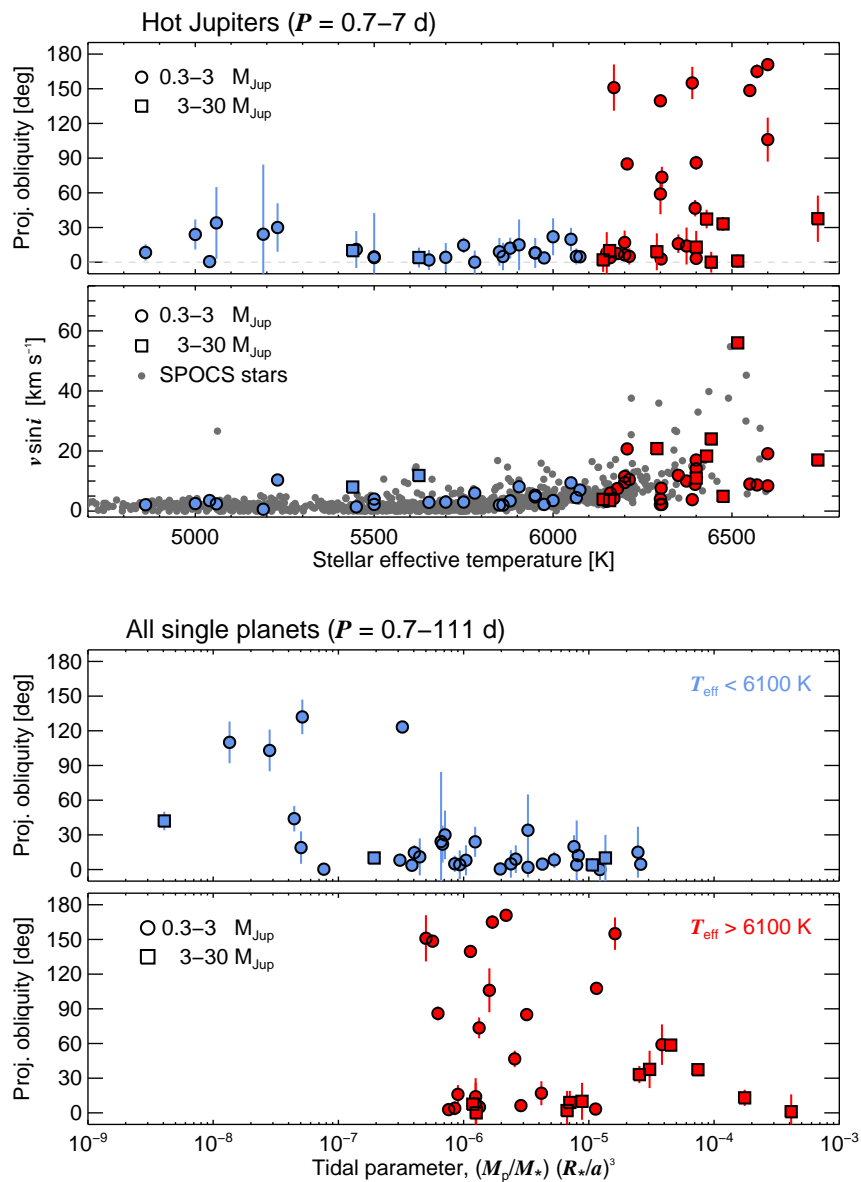


Figure 8 *Top.*—Sky-projected stellar obliquity and rotation velocity as a function of effective temperature, for “hot Jupiters” ( $M_p > 0.3 M_{\text{Jup}}$ ,  $P < 7$  days) with secure measurements. Planet mass is encoded by the symbol shape. Color is used to distinguish temperatures above and below 6100 K. Gray dots are projected rotation rates of stars in the SPOCS catalog (Valenti & Fischer 2005). *Bottom.*—Sky-projected stellar obliquity as a function of the relative strength of star-planet tidal forces, for all single-planet systems with secure measurements. These systems span a wider range of masses and orbital distances than the systems in the top panel.



Rossiter-McLaughlin effect is more difficult to observe for smaller and longer-period planets, new methods have been developed to gauge the stellar obliquity, some of which are more widely applicable or at least are suited to different types of systems:

1. In the  $v \sin i$  method, one divides estimates of  $v \sin i$  and  $v$  to obtain  $\sin i$ . If this is significantly smaller than unity for a star with a transiting planet, then the star has a high obliquity (Schlaufman 2010). Using this method, some candidate misaligned multitransiting systems have been identified (Walkowicz & Basri 2013, Hirano et al. 2014) but the results are uncertain because of the difficulty in measuring  $v \sin i$  for cool stars, the most common type of stellar host. Morton & Winn (2014) found a weak statistical tendency for multitransiting systems to have lower obliquities than the systems with only one known transiting planet.
2. The starspot-tracking method is based on events in which a transiting planet occults a starspot, temporarily reducing the loss of light and producing a glitch in the transit light curve. The obliquity can sometimes be decoded from a sequence of such anomalies (Sanchis-Ojeda et al. 2011, Désert et al. 2011). A related method relies on the correlations between the timing of a starspot-crossing event, and the phase of the corresponding flux modulation produced by the rotation of the starspot (Nutzman et al. 2011, Mazeh et al. 2014). Both methods were used to show that the stellar obliquity in the three-planet Kepler-30 system is  $\lesssim 10^\circ$  (Sanchis-Ojeda et al. 2012).
3. The starspot-variability method is based on the fact that the observed photometric variability due to rotating starspots should be larger for stars with  $\sin i \approx 1$  than for stars that are viewed more nearly pole-on. Mazeh et al. (2014) invented this technique and compared the photometric variability of *Kepler* stars with and without transiting planets. The relatively cool planet-hosting stars ( $\lesssim 5700$  K) showed greater variability than non-planet hosts, suggesting a tendency toward spin-orbit alignment.
4. The gravity-darkening method is based on transits across a rapidly-rotating star, which is darker near its equator because of the lifting and cooling effect of the centrifugal force. When the obliquity is high, this effect causes an asymmetry in the light curve (Barnes 2009), as seen during transits of Kepler-13 (Barnes et al. 2011, Szabo et al. 2011).
5. The asteroseismic method is based on the observed frequencies of stellar photospheric oscillations, which are classified by the usual “quantum numbers”  $nlm$ . For a non-rotating star, modes with the same  $nl$  and differing  $m$  are degenerate. Rotation splits the modes into multiplets. Crucially, the relative visibilities of the modes within each multiplet depend on viewing angle; the observed amplitudes thereby divulge the stellar obliquity (Gizon & Solanki 2003). The demanding observational requirements—years of ultraprecise photometry with  $\sim 1$  minute sampling—have only been met for a few *Kepler* stars. Chaplin et al. (2013) found low obliquities for two stars with multiple transiting planets (Kepler-50 and 65), and Van Eylen et al. (2014) found a low obliquity for the host of a Neptune-sized planet. On the other hand, Huber et al. (2013) found a  $45^\circ$  obliquity for the multiplanet system Kepler-56, and Benomar et al. (2014) found (with less confidence) a moderate obliquity for Kepler-25. These are the first sightings of spin-orbit misalignment for planets that seem distinct from hot Jupiters.

Obliquity, and its relation to planet formation, is a developing story. We await another round of clarification from a larger sample of more diverse systems, or the discovery of individually revealing cases. Regarding the latter, one of the most intriguing planetary

candidates is PTF0 8-8695 (van Eyken et al. 2012). This may be the first known case of a giant planet transiting a very young star ( $\lesssim 5$  Myr). In addition, the light curve changes shape on a timescale of months, a peculiarity which Barnes et al. (2013) attributed to nodal precession of a strongly misaligned orbit around the rapidly rotating, gravity-darkened star. Thus, this object may provide clues to the origin of high obliquities. However, the system has other strange and unsettling properties: the transit and stellar-rotation periods are both 16 hours (suggesting that starspots or accretion features may be causing the transit-like dimmings); the hypothetical planet would be at or within its Roche radius; giant planets on such short-period orbits are known to be rare around mature stars; and the planet’s Doppler signal cannot be detected in the face of the spurious variations produced by stellar activity. These factors cast doubt on the planetary interpretation, although the scientific stakes are high enough to warrant further investigation.

### 5.3 Star-disk alignment

We have focused on the alignment between a star’s equator and its planets’ orbital planes, but work has also been done on alignment with other planes, particularly the plane of a debris disk. Watson et al. (2011) used resolved images of debris disks and the  $v \sin i$  method to search for misalignments in 8 systems and found none greater than  $20\text{-}30^\circ$ . Greaves et al. (2014) added 10 systems observed with the *Herschel Space Observatory* and found alignment to within  $\lesssim 10^\circ$ . In contrast, there is mild evidence for a star-disk misalignment in the directly imaged system HR 8799, which has at least three giant planets at orbital distances of  $20\text{-}100$  AU. The debris disk has an inclination of  $26 \pm 3^\circ$  (Matthews et al. 2014), whereas the star has an inclination of  $\gtrsim 40^\circ$  according to the asteroseismic analysis by Wright et al. (2011a). Finally, in a technical *tour de force*, Le Bouquin et al. (2009) used optical interferometry to measure the position angle of the stellar equator of Fomalhaut b, showing it to be aligned within a few degrees of the debris disk.

## 6 BINARY STAR SYSTEMS

Although the Sun has no stellar companion, a substantial fraction of Sun-like stars are part of multiple-star systems (Raghavan et al. 2010). Naturally this makes one curious about the architecture of planetary systems with more than one star. In addition, investigating planets around stars with close stellar companions may help to clarify some aspects of planet-formation theory. The gravitational perturbations from a close companion would stir up the protoplanetary disk, complicating the process of building up large bodies from smaller ones. Whether or not planets manage to form despite these perturbations may provide a test of our understanding of this process (Thebault & Haghighipour 2014).

Almost all the literature on this topic deals with the effect of binary stars rather than systems of higher multiplicity. In that case, we may distinguish systems with planets orbiting one member of the binary from those with planets for which the orbit surrounds both members. In the nomenclature of Dvorak (1982) the former type of system is *S*-type (for satellite) and the latter is *P*-type (for planetary, although in this context a better term is circumbinary).

The three-body problem famously allows for chaos and instability, giving stringent restrictions on where we may find planetary orbits in binaries, regardless of how they formed. Holman & Wiegert (1999) used numerical integrations to explore these fundamental limits, as a function of the binary semimajor axis  $a_b$ , mass ratio, and orbital eccentricity. They

inserted a test particle (representing the planet) on an initially circular and prograde orbit, with varying orbital distances, and searched for the most extreme orbital distance  $a_c$  at which planets remained stable for  $10^4$  binary orbital periods. They provided useful fitting formulas for  $a_c$ , which can be summarized by the rough rule-of-thumb that the planet’s period should differ by at least a factor of three from the binary’s period, even for a mass ratio as low as 0.1. The zone of instability near the binary’s orbit widens for more massive secondaries or more eccentric binary orbits, as one would expect. These results were interpreted within the theory of resonance overlap by Mudryk & Wu (2006) and extended to noncoplanar orbits by Doolin & Blundell (2011).

### 6.1 Orbits around a single star

The Doppler surveys have been the main source of  $S$ -type planets. Approximately 70 examples are known (Roell et al. 2012), but only about 5 of these systems have separations  $\lesssim 50$  AU. These systems were typically recognized by detecting the planet through the Doppler method and then searching for additional stars through direct imaging or long-term Doppler monitoring (see, e.g., Eggenberger et al. 2007, Mugrauer et al. 2014). The selection effects are difficult to model because close binaries (with angular separations  $\lesssim 2''$ ) are avoided in the Doppler planet surveys, as it is difficult to achieve the necessary precision when the light from two stars is blended on the spectrograph.

Several investigators have tried to discern whether planet occurrence rates depend on the presence of a companion star. The broad synthesis of these studies is that for  $a_b \gtrsim 20$  AU, any such differences are small (Eggenberger et al. 2011). No planets are known in systems with smaller binary separations, which is at least partially due to selection bias. In no case has a planet been found with an orbit that is close to the stability limit  $a_c$ , or even within a factor of two. There is also an indication that for  $a_b \gtrsim 10^3$  AU, giant planets have slightly higher eccentricities (Kaib et al. 2013). In fact the four planets with the largest known eccentricities ( $e > 0.85$ ) are all members of  $S$ -type binaries (Tamuz et al. 2008).

Another approach is to search for stellar companions to *Kepler* planet-hosting stars, by following up with Doppler and direct imaging observations. This gives access to smaller planets than are usually found in the Doppler surveys but pays a penalty in sensitivity (and complexity of selection effects) as a result of the dilution of photometric transit signals by the light of the second star. Using this approach, Wang et al. (2014) found that binaries with  $a_b = 10\text{-}10^3$  AU have fewer planets than single stars by about a factor of two. This result pertains mainly to planets smaller than Neptune with periods of  $\lesssim 50$  days. At face value, then, the formation of these small close-in planets is somehow more sensitive to the presence of a companion star than the formation of giant planets found in Doppler surveys.

### 6.2 Orbits around two stars

$P$ -type planets are more exotic than  $S$ -type planets. They often appear in science fiction, with evocative scenes of alien double sunsets. The first known circumbinary planet was even more exotic than had been anticipated in science fiction: its host stars are a pulsar and a white dwarf (Thorsett et al. 1999). Based on the observed variations in the travel time of the radio pulses, caused by the pulsar’s orbital motion, it was possible to deduce that the pulsar B1620-26 has a white-dwarf companion in a 191 day orbit and that both are surrounded by a  $1\text{-}3 M_{\text{Jup}}$  companion with an orbital period of several decades (Sigurdsson et al. 2008). The system is in a globular cluster, and may have arisen through a dynamical exchange.

In this scenario the neutron star originally had a different white dwarf companion that was exchanged for a main-sequence star during a close encounter. A planet that was formerly orbiting the main-sequence star was cast into a circumbinary orbit, and eventually the main-sequence star evolved into the white dwarf seen today (Ford et al. 2000).

Timing the eclipses of other types of stellar binaries has led to the detection of candidate circumbinary planets, but with a less secure status than that of B1620-20. Within this category are about six cases of post-common-envelope binaries in which the observed eclipse timing variations are consistent with Keplerian motion induced by one or more circumbinary planets. Their properties and problems are reviewed by Horner et al. (2014). One serious problem is that in at least four cases, the proposed planetary orbits are dynamically unstable, casting doubt on the planetary hypothesis for those systems and leaving one wondering whether all the signals are the result of some other physical phenomenon. In one of the best studied systems, HU Aquarii, additional timing data refuted the planetary hypothesis (Bours et al. 2014), although the true origin of the timing variations is unknown.

The *Kepler* survey has led to the discovery of nine (and counting) transiting circumbinary planets around eclipsing binary stars. The detection of transits and the satisfactory fits of simple dynamical models to the observed transit and eclipse times leave very little room for doubt about the interpretation. In fact, because of the three-body effects, the dynamical models have in some cases provided unusually precise measurements of the masses and sizes of all three bodies (see, e.g., Doyle et al. 2011). Table 3 gives the basic properties of these systems, and Figure 9 depicts their orbital configurations. Kepler-47 is the only binary with more than one known planet (Orosz et al. 2012b, Kostov et al. 2013); in all the other cases, only one circumbinary planet is known in the system. A few trends are worth noting, though they are difficult to interpret at this stage:

1. The *Kepler* circumbinary planets all have sizes  $>3 R_{\oplus}$ . Smaller planets have not been excluded; they may simply be more difficult to detect. Unlike the case of isolated planets, it is not possible to build up the signal-to-noise ratio through simple period folding because the orbital motion of the stars causes substantial variations in the transit times and durations.
2. The planets seem to cluster just outside of the zone of instability (see the lower right panel of Fig. 9). Such a pile-up had been predicted by theoreticians as a consequence of migration of giant planets within a circumbinary disk (Pierens & Nelson 2008). Here as always, though, lurks the specter of selection effects: the transit method favors the detection of planets with the shortest possible periods.
3. The binary and planetary orbits are aligned to within a few degrees, as seen in Fig. 9. This too may be a selection effect: it is easier to recognize planets when multiple transits are detected, as is often the case in coplanar systems but not in inclined systems. We await the unambiguous discovery of circumbinary planets through methods that are less biased with respect to orbital coplanarity, such as eclipse timing variations (Borkovits et al. 2011) or transits of non-eclipsing binaries (Martin & Triaud 2014).

As with *S*-type planets, it is interesting to compare the occurrence rate for circumbinary planets with that of single-star planets. This is not straightforward because the geometric transit probability depends on the binary properties as well as the inclination between the two orbital planes. Furthermore, precession of noncoplanar systems causes the existence of transits to be ephemeral. A particular system may display transits for a few months and then cease for years before displaying them again (Schneider 1994, Kostov et al. 2013).

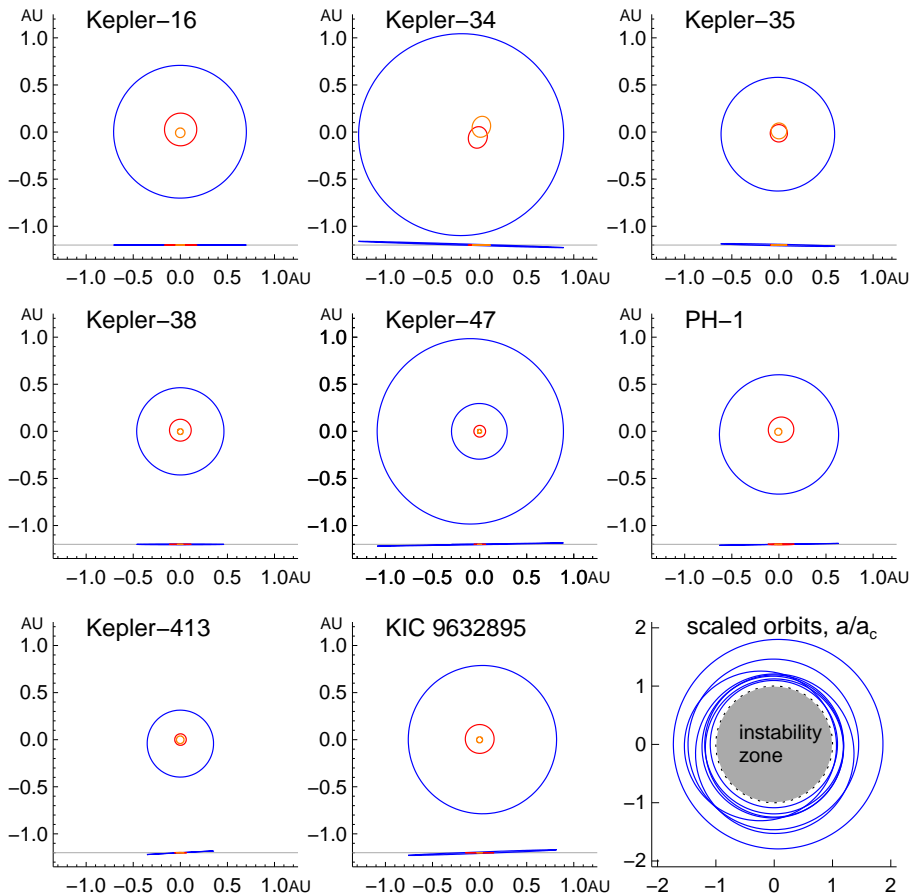


Figure 9 Gallery of the *Kepler* circumbinary planetary systems. Each panel has the same scale. Orange orbits are for the primary stars, red are for the secondary stars, and blue are for the planets. Near the bottom of each panel, a side view is shown, with the gray line indicating the stellar orbital plane. In the bottom right panel, the orbits are scaled to the size of the critical semi-major axis for stability ( $a_c$ ) as estimated from the equations by Holman & Wiegert (1999). The planets seem to bunch just outside the instability zone (although Kepler-47’s exterior planet is too distant to fit in this plot).

Despite these difficulties, Armstrong et al. (2014) attempted to calculate the occurrence rate of circumbinary planets. They evaluated the observability of circumbinary planets within the sample of *Kepler* eclipsing binaries and tested for consistency between the currently-detected systems and various proposed planet distributions. They favored a model in which around 10% of binaries host a  $6\text{--}10 R_{\oplus}$  planet on a nearly coplanar orbit ( $\Delta i \lesssim 5^\circ$ ) somewhere between the stability limit and an outer period of 300 days. This fraction of  $\approx 10\%$  is consistent with the rates seen around single stars (Table 1). The implication is that  $\gtrsim 6 R_{\oplus}$  planets populate the space  $\lesssim 1$  AU just as readily around binaries as single stars. However, when they allowed for the possibility of noncoplanar orbits, no firm conclusion could be reached owing to a degeneracy between coplanarity and multiplicity.

Table 3. Key properties of *Kepler* circumbinary planets

Name	$M_A$ [ $M_\odot$ ]	$M_B$ [ $M_\odot$ ]	$P_{\text{bin}}$ [days]	$e_{\text{bin}}$	$M_p$ [ $M_{\text{Jup}}$ ]	$P_p$ [days]	$e_p$	$i_{\text{mut}}$ ( $^\circ$ )	$P_p/P_c$	Ref.
Kepler-16b	0.690	0.203	41.07922	0.1594	0.333	228.776	0.0069	0.3	1.14	1
Kepler-34b	1.0479	1.0208	27.79581	0.5209	0.220	288.822	0.182	1.8	1.21	2
Kepler-35b	0.8877	0.8094	20.73367	0.1421	0.127	131.458	0.042	1.3	1.24	2
Kepler-38b	0.941	0.248	18.79537	0.1042	< 0.2	105.599	0.0	0.2	1.42	3
Kepler-47b	1.043	0.362	7.44838	0.0234	< 0.1	49.514	0.01	0.3	1.77	4
Kepler-47c	1.043	0.362	7.44838	0.0234	< 0.1	303.158	0.1	1.1	10.8	4
PH-1b	1.384	0.386	20.00021	0.2117	< 0.1	138.506	0.052	2.8	1.29	5
Kepler-413b	0.820	0.542	10.11615	0.037	< 0.1	66.262	0.117	4.1	1.60	6
KIC 9632895b	0.934	0.194	27.32204	0.0510	< 0.1	240.503	0.038	2.3	2.41	7

Note. — In column 10,  $P_c$  refers to the critical orbital period, the minimum period compatible with long-term stability according to the equations of Holman & Wiegert (1999). References: (1) Doyle et al. (2011), (2) Welsh et al. (2012), (3) Orosz et al. (2012a), (4) Orosz et al. (2012b), (5) Schwamb et al. (2013), (6) Kostov et al. (2013), (7) Welsh et al. (2014).

An interesting trend is that when the *Kepler* eclipsing binaries are sorted in order of orbital period, all eight circumbinary-planet hosts are found among the longer-period half. This does not seem to be purely a selection effect (Armstrong et al. 2014, Martin & Triard 2014). This observation, if confirmed by additional analysis, would support the theory that very close binary stars ( $\lesssim 5$  days) form through a different mechanism than wider binaries. Specifically, they may be the product of orbital shrinkage due to gravitational perturbations from a third wide-orbiting star and the long-term effect of tidal dissipation (Mazeh & Shaham 1979, Fabrycky & Tremaine 2007). The perturbations and the shrinkage process would likely be hostile to circumbinary planets, preventing their formation or putting them at risk of ejection or accretion onto the stars. This would be a delightful example of an advance in exoplanetary science leading to progress in star-formation theory.

## 7 SUMMARY AND DISCUSSION

Over the past few decades, astronomers have gradually become aware of the following properties of planets around other stars:

- A Sun-like star has a  $\approx 10\%$  chance of having a giant planet with a period shorter than a few years, and a  $\approx 50\%$  chance of having a compact system of smaller planets with periods shorter than a year.
- The giant planets have a broad eccentricity distribution, ranging from around 0–0.9 with a mean of  $\approx 0.2$ . The smaller planets have lower eccentricities ( $\lesssim 0.1$ ), particularly those in multiplanet systems.
- In compact systems of small planets, the orbits are typically aligned to within a few degrees. Giant planets may occasionally have larger mutual inclinations.
- The ratios of orbital periods are often in the range of 2–3 but are occasionally closer to unity, flirting with instability.
- Giant planets are more often found in mean-motion resonances than smaller planets, which show only a slight preference for being near resonances.

- The stellar rotation axis can be grossly misaligned with the planetary orbital axis, particularly for close-in giant planets orbiting relatively hot stars ( $T_{\text{eff}} \gtrsim 6100$  K);
- Close binary stars host circumbinary giant planets just outside of the zone of instability, with an occurrence rate comparable with that of giant planets at similar orbital distances around single stars.

We are now in a position to compare this exoplanetary list with that given for the Solar System (§ 1). The hope has always been that such a comparison would help answer one of the big questions of exoplanetary science: How do planets form? We discuss this question in § 7.1, but limit ourselves to broad-brush remarks. One important difference to keep in mind is that the Solar System properties are indisputable and provide a fairly complete picture. In contrast the exoplanetary list is provisional and based on the myopic views of planetary systems that are inherent to existing astronomical techniques. In § 7.2 we review the prospects for obtaining a clearer picture.

## 7.1 Planet-formation theory

By the mid-1990s the prevailing theoretical paradigm for planet formation was that planets originate from the coagulation of very small solid bodies. Although this notion cannot be traced back to Laplace’s theory, in which planets formed from gaseous rings, it is nevertheless an old idea, dating back at least to Chamberlin (1916) who called it the “planetesimal hypothesis.” Between the 1960s and 1990s many theorists turned this hypothesis into a detailed mechanistic theory, which included the further realization that a large enough solid body could undergo runaway accretion of gas and become a giant planet, a phenomenon that has become known as “core accretion” (Mizuno 1980, Pollack et al. 1996).

The main predictions of this theory for the geometrical properties of exoplanetary systems were that the eccentricities and inclinations should be low. The inclinations are low because the processes take place within a flat disk. The eccentricities are low because the streamlines within the disk are nearly circular; this is a consequence of viscous dissipation. Furthermore, even if an object managed to acquire a moderate eccentricity or inclination, gravitational and hydrodynamical interactions with the disk would coplanarize and circularize its orbit (Cresswell et al. 2007, Xiang-Gruess & Papaloizou 2013). The theory also predicted that a planet’s composition should be linked to the location of its formation within the disk. Giant planets, in particular, would be found beyond the “snow line” at a few astronomical units, where water exists as a solid, enhancing the abundance of solid material and promoting rapid accretion. These predictions were taken seriously enough that HD 114762b, now understood as a short-period giant planet on an eccentric orbit, was not recognized as an exoplanet at the time of its discovery in 1989 (Latham 2012).

Even the most grotesque violations of these expectations—high eccentricities, retrograde orbits, extremely short-period giant planets—have not shattered the paradigm of planet-formation theory. The only other theory that is occasionally discussed is gravitational instability, in which the gaseous disk collapses directly into giant planets (Boss 1997). However, this theory leads to essentially the same predictions for low eccentricities and inclinations as does core accretion. Criticism of gravitational instability has been mainly on non-geometric grounds, such as whether the thermodynamic properties of the disk allow for collapse, and whether the theory is compatible with the correlation between metallicity and giant-planet occurrence (as reviewed by Durisen et al. 2007).

The failure of planet-formation theory to anticipate the geometric properties of exoplane-

tary systems is generally understood as a failure to pay attention to what may happen after planets form. Attention had been focused too narrowly on the conglomeration of solid material and the accretion of gas. Now, more attention is paid to the interactions of the cores and planets with each other and with the protoplanetary disk while it still exists. Gravitational interactions with the disk can cause a planet to spiral inward or “migrate” (Lin et al. 1996, Ward et al. 1997), possibly explaining the close-in giant planets. High eccentricities and inclinations can be generated by resonant interactions with the disk (Goldreich & Sari 2003, D’Angelo et al. 2006, Bitsch et al. 2013), or between planets (Thommes & Lissauer 2003). They can also be generated independently of the disk, through planet-planet scattering (see, e.g., Chatterjee et al. 2008), or torquing from a distant massive companion (Fabrycky & Tremaine 2007).

The closest we have seen to an attempt at paradigm shift is the proposal that the small low-density planets within compact systems formed essentially at the locations where they are seen today, rather than having migrated inward from the snow line or beyond (Raymond et al. 2008, Hansen & Murray 2012, Chiang & Laughlin 2013). This would require the protoplanetary disk to have surface density approximately ten times higher than is commonly thought. However, disk migration theory also seems capable of explaining the formation of these systems (Terquem & Papaloizou 2007). Disks have fluid, thermodynamic, and electromagnetic properties of potentially crucial importance that are poorly understood. From an observer’s perspective there seem to be few observations that cannot be accommodated by adjusting the properties of the disk.

In short, the survival of the planetesimal hypothesis and core accretion theory after the onslaught of exoplanetary data may be a sign that the theory is correct, if lacking in some details. However, it may also partially reflect the deep entrenchment of the theory after having enjoyed a very long interval of time when the only known planets were inside the Solar System. We wish we could travel back in time to 1795, deliver this manuscript to Laplace, and follow the subsequent development of planet-formation theory.

## 7.2 Future observations

The Doppler and transit techniques have provided a fairly detailed description of the inner regions of planetary systems. We may now look forward to similar information about the outer regions of exoplanetary systems as the astrometric, microlensing, and direct imaging techniques reach greater maturity in the coming decade.

Astrometry has had little impact on exoplanetary science beyond a few detections of previously-known planets (Benedict et al. 2002) and spurious detections of new planets (see, e.g., Pravdo & Shaklan 2009, whose claim was refuted by Bean et al. 2010). The European *Gaia* mission should improve this situation. Casertano et al. (2008) forecasted that the  $\approx 5 \mu\text{s}$  precision of *Gaia*’s positional measurements would lead to thousands of detections of giant planets with orbits out to 3-4 AU. Astrometry also exposes the full three-dimensional orbits of planets, apart from a twofold degeneracy (an orbit cannot be distinguished from its sky-plane mirror reflection). Thus, for some *Gaia* multiplanet systems, it should be possible to measure mutual inclinations. In addition *Gaia* will search for planets around massive stars, evolved stars, young stars, and other types of stars that misbehave in Doppler and transit surveys but are more cooperative in astrometric surveys.

Microlensing has already made substantial contributions and is poised to offer more. The Korean Microlensing Telescope Network plans to use three dedicated 1.6-m telescopes to perform a dedicated survey with nearly continuous time coverage (Park et al. 2012).



The completed network—scheduled to begin operation in 2015—is predicted to find  $\approx 60$  planets year<sup>-1</sup> ranging in mass from 0.1 to  $10^3 M_{\oplus}$  and in orbital distance from 0.4 to 16 AU (Henderson et al. 2014). An even more prodigious planet discovery rate could be achieved with a space telescope (Bennett & Rhie 2002), such as the 2.4-m wide-field infrared telescope currently being planned for both cosmology and exoplanetary science. The mission’s name fluctuates; at the time of writing, it is *WFIRST-AFTA*. Barry et al. (2011) predicted that this survey will detect thousands of planets with orbital distances of a few AU, thereby complementing *Kepler*’s view of sub-AU systems. It will be a challenge to extract any architectural information from these systems beyond the instantaneous sky-projected orbital separations.

Direct imaging detections have been relatively few and limited to massive planets with orbital distances  $\gtrsim 20$  AU, but the technique is flourishing with the advent of new high-contrast imagers for large ground-based telescopes (Beuzit et al. 2008, Close et al. 2014, Macintosh et al. 2014, Jovanovic et al. 2014). These are expected to provide an order-of-magnitude improvement in contrast, enabling hundreds of young stars to be searched for giant planets. In addition, the Atacama Large Millimeter Array has enabled direct imaging of the inner regions of gaseous protoplanetary disks, which may reveal structures associated with planet formation. Biller et al. (2014) and Reggiani et al. (2014) recently detected a “blob” that may represent such a structure. Further ahead, *WFIRST-AFTA* may have a coronagraph capable of detecting planets analogous to the Solar System’s giant planets.

Even though the Doppler and transit techniques have already reached a high level of maturity, they show no signs of exhaustion. Numerous new Doppler instruments are planned, with the goal of detecting habitable-zone Earth-mass planets. They include traditional optical spectrographs well suited for FGK dwarfs (Pepe et al. 2010, Szentgyorgyi et al. 2012, Pasquini et al. 2008) as well as new infrared spectrographs more appropriate for M dwarfs (Tamura et al. 2012, Quirrenbach et al. 2010, Mahadevan et al. 2012, Delfosse et al. 2013). The main attraction of M dwarfs is that the habitable zone occurs at shorter orbital distances, expediting planet searches.

The sky will continue to be scoured for transiting planets. A new round of ground-based surveys is underway, aiming to extend the hunt beyond their traditional quarry of hot Jupiters into the realm of Neptune-sized planets (Bakos et al. 2013, Wheatley et al. 2013), or even smaller planets around M dwarfs (Nutzman & Charbonneau 2008, Giacobbe et al. 2012, Gillon et al. 2013). In space, the handicapped but still potent *Kepler* telescope has begun monitoring several star fields near the ecliptic plane, the only zone in which it can achieve stable pointing (Howell et al. 2014). The European *Characterising Exoplanet Satellite (CHEOPS)* mission (Broeg et al. 2013) aims to achieve precise photometry for bright stars, search for transits of Doppler planets, and improve upon the light curves of previously detected transiting planets. NASA’s *Transiting Exoplanet Survey Satellite (TESS)* is scheduled to perform an all-sky, bright-star survey for short-period transiting planets in 2018-2019 (Ricker et al. 2015). Further out, in the mid-to-late 2020s, the European *Planetary Transits and Oscillations (PLATO)* mission intends to begin longer-duration transit survey over half of the celestial sphere (Rauer et al. 2014).

The continued analysis of *Kepler* data may reveal the architectures of additional systems through the measurement and interpretation of transit-timing variations. Long-period companions in those systems may be revealed through long-term Doppler observations and *Gaia* astrometry. The current and forthcoming transit data may also reveal planetary satellite systems, or planetary rotation rates and obliquities, which are interesting features of the Solar System but are essentially unknown for exoplanets. Current satellite searches are

limited to relatively large companions around approximately a dozen of the most observationally favorable planets (Kipping 2014). A wildcard possibility is the discovery of the third category of three-body system classified by (Dvorak 1982), the so-called  $L$ -type (“librator”). This would be a Trojan companion to a planet, one whose orbit surrounds the  $L_4$  and  $L_5$  Lagrange points of the star-planet system ( $60^\circ$  ahead or behind the planet’s orbit). As for planetary spin, the only successful measurement to date has been from direct imaging: Snellen et al. (2014) found the giant planet around  $\beta$  Pic to be spinning more rapidly than any Solar System planet ( $v \sin i = 25 \pm 3 \text{ km s}^{-1}$ , as compared to  $13 \text{ km s}^{-1}$  for Jupiter). This finding was based on the Doppler broadening of the planet’s spectrum.

Clearly there is vast scope for improving our understanding of the occurrence and architecture of exoplanetary systems. Still, it seems appropriate to admire the progress that has been made. Consider again the thought experiment of traveling back in time to deliver this information to Laplace. With so many startling results, it is difficult to guess what would have impressed him the most: the high eccentricities, the retrograde planets, the chaotic systems, the circumbinary systems; the ceaseless technological developments that have propelled the field; or the mere fact that we have learned so much about faraway planetary systems on the basis of only the minuscule changes in brightness and color of points of light?

## 8 DISCLOSURE STATEMENT

The authors are not aware of any affiliations, memberships, funding, or financial holdings that might be perceived as affecting the objectivity of this review.

## 9 ACKNOWLEDGMENTS

We are grateful to Eric Agol, Simon Albrecht, Eric Ford, Jonathan Fortney, Andrew Howard, Jack Lissauer, Scott Tremaine, Amaury Triaud, Bill Welsh, and Liang Yu for helpful comments on the manuscript. J.N.W. thanks Avi Loeb, Matt Holman, and the Institute for Theory and Computation at the Harvard-Smithsonian Center for Astrophysics for their hospitality while this review was written. D.C.F. thanks the Kepler TTV/Multis and Eclipsing Binary groups for sharing an interesting scientific journey, as well as University of Chicago students and postdocs for sharpening his thoughts on these topics. This work was supported by funding from the NASA Origins program (NNX11AG85G) and Kepler Participating Scientist program (NNX12AC76G, NNX14AB87G).

### LITERATURE CITED

- Adibekyan VZ, Figueira P, Santos NC, Mortier A, Mordasini C, et al. 2013. *Astron. Astrophys.* 560:A51
- Agol E, Steffen J, Sari R, Clarkson W. 2005. *MNRAS* 359:567–579
- Aigrain S, Collier Cameron A, Ollivier M, Pont F, Jorda L, et al. 2008. *Astron. Astrophys.* 488:L43–L46
- Albrecht S, Winn JN, Johnson JA, Howard AW, Marcy GW, et al. 2012. *Ap. J.* 757:18
- Alves S, Do Nascimento Jr. JD, de Medeiros JR. 2010. *MNRAS* 408:1770–1777
- Armstrong DJ, Osborn HP, Brown DJA, Faedi F, Gómez Maqueo Chew Y, et al. 2014. *MNRAS* 444:1873–1883
- Bakos GÁ, Csabry Z, Penev K, Bayliss D, Jordán A, et al. 2013. *Pub. Astron. Soc. Pac.* 125:154–182
- Ballard S, Johnson JA. 2014. Submitted to *Ap. J.*, [arxiv:1410.4192](https://arxiv.org/abs/1410.4192)

- Ballard S, Fabrycky D, Fressin F, Charbonneau D, Desert JM, et al. 2011. *Ap. J.* 743:200
- Baluev RV. 2011. *Celestial Mechanics and Dynamical Astronomy* 111:235–266
- Barnes JW. 2009. *Ap. J.* 705:683–692
- Barnes SA. 2001. *Ap. J.* 561:1095–1106
- Barnes JW, Linscott E, Shporer A. 2011. *Ap. J. Suppl.* 197:10
- Barnes JW, van Eyken JC, Jackson BK, Ciardi DR, Fortney JJ. 2013. *Ap. J.* 774:53
- Barry R, Kruk J, Anderson J, Beaulieu JP, Bennett DP, et al. 2011. In *Techniques and Instrumentation for Detection of Exoplanets V*, ed. S Shaklan. *Proc. SPIE Conf. Ser.* 8151:815110L. Bellingham, WA: SPIE
- Bate MR, Lodato G, Pringle JE. 2010. *MNRAS* 401:1505–1513
- Batygin K, Morbidelli A. 2013. *Astron. J.* 145:1
- Batygin K, Morbidelli A, Tsiganis K. 2011. *Astron. Astrophys.* 533:A7
- Bayliss DDR, Sackett PD. 2011. *Ap. J.* 743:103
- Bean JL, Seifahrt A. 2009. *Astron. Astrophys.* 496:249–257
- Bean JL, Seifahrt A, Hartman H, Nilsson H, Reiners A, et al. 2010. *Ap. J. Let.* 711:L19–L23
- Benedict GF, McArthur BE, Forveille T, Delfosse X, Nelan E, et al. 2002. *Ap. J. Let.* 581:L115–L118
- Bennett DP, Rhie SH. 2002. *Ap. J.* 574:985–1003
- Benomar O, Masuda K, Shibahashi H, Suto Y. 2014. *Publ. Astron. Soc. Japan*, 10.1093/pasj/psu069
- Beuzit JL, Feldt M, Dohlen K, Mouillet D, Puget P, et al. 2008. In *Ground-Based and Airborne Instrumentation for Astronomy II*, ed. IS McLean, MM Casali. *Proc. SPIE Conf. Ser.* 7014:701418. Bellingham, WA: SPIE
- Billar BA, Liu MC, Wahhaj Z, Nielsen EL, Hayward TL, et al. 2013. *Ap. J.* 777:160
- Billar BA, Males J, Rodigas T, Morzinski K, Close LM, et al. 2014. *Ap. J. Let.* 792:L22
- Bitsch B, Crida A, Libert AS, Lega E. 2013. *Astron. Astrophys.* 555:A124
- Bonfils X, Delfosse X, Udry S, Forveille T, Mayor M, et al. 2013. *Astron. Astrophys.* 549:A109
- Borkovits T, Csizmadia S, Forgács-Dajka E, Hegedüs T. 2011. *Astron. Astrophys.* 528:A53
- Borucki WJ, Agol E, Fressin F, Kaltenegger L, Rowe J, et al. 2013. *Science* 340:587–590
- Boss AP. 1997. *Science* 276:1836–1839
- Bours M, Marsh T, Breedt E, Copperwheat C, Dhillon V, et al. 2014. *MNRAS* 445:1924
- Brandt TD, Kuzuhara M, McElwain MW, Schlieder JE, Wisniewski JP, et al. 2014. *Ap. J.* 786:1
- Broeg C, Fortier A, Ehrenreich D, Alibert Y, Baumjohann W, et al. 2013. In *European Physical Journal Web of Conferences*, 47:3005
- Brown DJA, Collier Cameron A, Hall C, Hebb L, Smalley B. 2011. *MNRAS* 415:605–618
- Brown DJA. 2014. *MNRAS* 442:1844–1862
- Buchhave LA, Latham DW, Johansen A, Bizzarro M, Torres G, et al. 2012. *Nature* 486:375–377
- Burke C. 2008. *Ap. J.* 679:1566–1573
- Burke CJ, Bryson ST, Mullally F, Rowe JF, Christiansen JL, et al. 2014. *Ap. J. Suppl.* 210:19
- Butler RP, Marcy GW, Williams E, Hauser H, Shirts P. 1997. *Ap. J. Let.* 474:L115–L118
- Butler RP, Vogt SS, Marcy GW, Fischer DA, Wright JT, et al. 2004. *Ap. J.* 617:580–588
- Carney BW, Aguilar LA, Latham DW, Laird JB. 2005. *Astron. J.* 129:1886–1905
- Carter JA, Agol E, Chaplin WJ, Basu S, Bedding TR, et al. 2012. *Science* 337:556–
- Casertano S, Lattanzi MG, Sozzetti A, Spagna A, Jancart S, et al. 2008. *Astron. Astrophys.* 482:699–729
- Cassan A, Kubas D, Beaulieu JP, Dominik M, Horne K, et al. 2012. *Nature* 481:167–169
- Catanzarite J, Shao M. 2011. *Ap. J.* 738:151
- Chamberlin TC. 1916. *J. R. Astron. Soc. Canada* 10:473
- Chaplin WJ, Sanchis-Ojeda R, Campante TL, Handberg R, Stello D, et al. 2013. *Ap. J.* 766:101
- Chatterjee S, Ford EB. 2015. *Ap. J.* 803:33
- Chatterjee S, Ford EB, Matsumura S, Rasio FA. 2008. *Ap. J.* 686:580–602
- Chiang E, Laughlin G. 2013. *MNRAS* 431:3444–3455
- Clanton C, Gaudi BS. 2014. *Ap. J.* 791:91

- Close LM, Males JR, Follette KB, Hinz P, Morzinski KM, et al. 2014. In *Adaptive Optics Systems IV*, ed. E Marchetti, LM Close, J-P Véran. *Proc. SPIE Conf. Ser.* 9148:91481M. Bellingham, WA: SPIE
- Correia ACM, Couetdic J, Laskar J, Bonfils X, Mayor M, et al. 2010. *Astron. Astrophys.* 511:A21
- Counselman III CC. 1973. *Ap. J.* 180:307–316
- Cresswell P, Dirksen G, Kley W, Nelson RP. 2007. *Astron. Astrophys.* 473:329–342
- Cumming A, Butler RP, Marcy GW, Vogt SS, Wright JT, Fischer DA. 2008. *Pub. Astron. Soc. Pac.* 120:531–554
- D’Angelo G, Lubow SH, Bate MR. 2006. *Ap. J.* 652:1698–1714
- Dawson RI. 2014. *Ap. J. Let.* 790:L31
- Dawson RI, Chiang E. 2014. *Science* 346:212–
- Dawson RI, Johnson JA. 2012. *Ap. J.* 756:122
- Dawson RI, Johnson JA, Fabrycky DC, Foreman-Mackey D, Murray-Clay RA, et al. 2014. *Ap. J.* 791:89
- Dawson RI, Murray-Clay RA. 2013. *Ap. J. Let.* 767:L24
- Deck KM, Holman MJ, Agol E, Carter JA, Lissauer JJ, et al. 2012. *Ap. J. Let.* 755:L21
- Delfosse X, Donati JF, Kouach D, Hébrard G, Doyon R, et al. 2013. In *SF2A-2013: Proceedings of the Annual meeting of the French Society of Astronomy and Astrophysics*, eds. L Cambresy, F Martins, E Nuss, A Palacios, June 4–7, pp. 497–508
- Désert JM, Charbonneau D, Demory BO, Ballard S, Carter JA, et al. 2011. *Ap. J. Suppl.* 197:14
- Dong S, Zhu Z. 2013. *Ap. J.* 778:53
- Dong S, Katz B., Socrates A. 2014. *Ap. J. Let.* 781:L5
- Doolin S, Blundell KM. 2011. *MNRAS* 418:2656–2668
- Doyle LR, Carter JA, Fabrycky DC, Slawson RW, Howell SB, et al. 2011. *Science* 333:1602
- Dressing CD, Charbonneau D. 2013. *Ap. J.* 767:95
- Durisen RH, Boss AP, Mayer L, Nelson AF, Quinn T, Rice WKM. 2007. In *Protostars and Planets V*, eds. Reipurth B, Jewitt D, Keil K, University of Arizona Press (Tucson), 607–622
- Dvorak R. 1982. *Oesterreichische Akademie Wissenschaften Mathematisch naturwissenschaftliche Klasse Sitzungsberichte Abteilung* 191:423–437
- Eggenberger A, Udry S, Chauvin G, Beuzit JL, Lagrange AM, et al. 2007. *Astron. Astrophys.* 474:273–291
- Eggenberger A, Udry S, Chauvin G, Forveille T, Beuzit JL, et al. 2011. In *Proc. IAU Symp. 276*, ed. A Sozzetti, MG Lattanzi, AP Boss, pp. 409–10. Cambridge, UK: Cambridge Univ. Press
- Endl M, Cochran WD, Kürster M, Paulson DB, Wittenmyer RA, et al. 2006. *Ap. J.* 649:436–443
- Fabrycky D, Tremaine S. 2007. *Ap. J.* 669:1298–1315
- Fabrycky DC, Murray-Clay RA. 2010. *Ap. J.* 710:1408–1421
- Fabrycky DC, Lissauer JJ, Ragozzine D, Rowe JF, Steffen JH, et al. 2014. *Ap. J.* 790:146
- Fang J, Margot JL. 2012. *Ap. J.* 761:92
- Fielding DB, McKee CF, Socrates A, Cunningham AJ, Klein RI. 2014. Submitted to *MNRAS*, [arxiv:1409.5148](https://arxiv.org/abs/1409.5148)
- Figueira P, Marmier M, Boué G, Lovis C, Santos NC, et al. 2012. *Astron. Astrophys.* 541:A139
- Ford EB. 2014. *Proc. Nat. Acad. Sci.* 111:12616
- Ford EB, Rasio FA. 2008. *Ap. J.* 686:621–636
- Ford EB, Quinn SN, Veras D. 2008. *Ap. J.* 678:1407–1418
- Ford EB, Joshi KJ, Rasio FA, Zbarsky B. 2000. *Ap. J.* 528:336–350
- Foreman-Mackey D, Hogg DW, Morton TD. 2014. *Ap. J.*, 795:64
- Fressin F, Torres G, Charbonneau D, Bryson ST, Christiansen J, et al. 2013. *Ap. J.* 766:81
- Gaudi BS, Bennett DP, Udalski A, Gould A, Christie GW, et al. 2008. *Science* 319:927
- Giacobbe P, Damasso M, Sozzetti A, Toso G, Perdoncin M, et al. 2012. *MNRAS* 424:3101–3122
- Gillon M, Jehin E, Delrez L, Magain P, Opitom C, Sohy S. 2013. In *Protostars and Planets VIII Posters*, <http://www.mpia-hd.mpg.de/homes/ppvi/posters/2K066.html>
- Gizon L, Solanki SK. 2003. *Ap. J.* 589:1009–1019

Goldreich P, Sari R. 2003. *Ap. J.* 585:1024–1037

Goldreich P, Schlichting HE. 2014. *Astron. J.* 147:32

Goldreich P, Soter S. 1966. *Icarus* 5:375–389

Goldreich P, Tremaine S. 1980. *Ap. J.* 241:425–441

Gonzalez G. 1997. *MNRAS* 285:403–412

Gonzalez G. 2011. *MNRAS* 416:L80–L83

Gould A, Dong S, Gaudi BS, Udalski A, Bond IA, et al. 2010. *Ap. J.* 720:1073–1089

Gould A, Dorsher S, Gaudi BS, Udalski A. 2006. *Acta Astronomica* 56:1–50

Goździewski K, Migaszewski C. 2014. *MNRAS* 440:3140–3171

Greaves JS, Kennedy GM, Thureau N, Eiroa C, Marshall JP, et al. 2014. *MNRAS* 438:L31–L35

Grether D, Lineweaver CH. 2006. *Ap. J.* 640:1051–1062

Grether D, Lineweaver CH. 2007. *Ap. J.* 669:1220–1234

Guedel M, Dvorak R, Erkaev N, Kasting J, Khodachenko M, et al. 2014. In *Protostars and Planets VI*, eds. H Beuther, RS Klessen, CP Dullemond, T Henning. Tucson: Univ. Ariz. Press, p. 883906

Han C, Udalski A, Choi JY, Yee JC, Gould A, et al. 2013. *Ap. J. Let.* 762:L28

Hansen BMS, Murray N. 2012. *Ap. J.* 751:158

Hansen BMS, Murray N. 2013. *Ap. J.* 775:53

Hayes W, Tremaine S. 1998. *Icarus* 135:549–557

Hébrard G, Bouchy F, Pont F, Loeillet B, Rabus M, et al. 2008. *Astron. Astrophys.* 488:763–770

Hébrard G, Désert JM, Díaz RF, Boisse I, Bouchy F, et al. 2010. *Astron. Astrophys.* 516:A95

Hébrard G, Ehrenreich D, Bouchy F, et al. 2011. *Astron. Astrophys.* 527:L11

Henderson CB, Gaudi BS, Han C, Skowron J, Penny MT, et al. 2014. *Ap. J.* 794:52

Heisler J, Tremaine S. 1986. *Icarus* 65:13–26

Hirano T, Narita N, Sato B, Winn JN, Aoki W, et al. 2011. *PASJ* 63:L57–L61

Hirano T, Narita N, Sato B, Takahashi YH, Masuda K, et al. 2012. *Ap. J. Let.* 759:L36

Hirano T, Sanchis-Ojeda R, Takeda Y, Winn JN, Narita N, Takahashi YH. 2014. *Ap. J.* 783:9

Hogg DW, Myers AD, Bovy J. 2010. *Ap. J.* 725:2166–2175

Holman MJ, Fabrycky DC, Ragozzine D, Ford EB, Steffen JH, et al. 2010. *Science* 330:51

Holman MJ, Murray NW. 2005. *Science* 307:1288–1291

Holman MJ, Wiegert PA. 1999. *Astron. J.* 117:621–628

Horner J, Wittenmyer R, Hinse T, Marshall J, Mustill A. 2014. To appear in *Proc. Australian Space Science Conf.*, [arxiv:1401:6742](https://arxiv.org/abs/1401.6742)

Howard AW, Marcy GW, Bryson ST, Jenkins JM, Rowe JF, et al. 2012. *Ap. J. Suppl.* 201:15

Howard AW, Marcy GW, Johnson JA, Fischer DA, Wright JT, et al. 2010. *Science* 330:653

Howell SB, Sobek C, Haas M, Still M, Barclay T, et al. 2014. *Pub. Astron. Soc. Pac.* 126:398–408

Huber D, Carter JA, Barbieri M, Miglio A, Deck KM, et al. 2013. *Science* 342:331–334

Husnoo N, Pont F, Mazeh T, Fabrycky D, Hébrard G, et al. 2012. *MNRAS* 422:3151–3177

Hut P. 1980. *Astron. Astrophys.* 92:167–170

Jeans JH. 1942. *Nature* 149:695

Ji J, Li G, Liu L. 2002. *Ap. J.* 572:1041–1047

Johansen A, Davies MB, Church RP, Holmelin V. 2012. *Ap. J.* 758:39

Johnson JA, Aller KM, Howard AW, Crepp JR. 2010. *Pub. Astron. Soc. Pac.* 122:905–915

Johnson JA, Butler RP, Marcy GW, Fischer DA, Vogt SS, et al. 2007. *Ap. J.* 670:833–840

Johnson JA, Marcy GW, Fischer DA, Henry GW, Wright JT, et al. 2006. *Ap. J.* 652:1724–1728

Jovanovic N, Guyon O, Martinache F, Clergeon C, Singh G, et al. 2014. In *Ground-Based and Airborne Instrumentation for Astronomy V*, ed. SK Ramsay, IS McLean, H Takami. *Proc. SPIE Conf. Ser.* 9147:91471Q

Jurić M, Tremaine S. 2008. *Ap. J.* 686:603–620

Kaib NA, Raymond SN, Duncan M. 2013. *Nature* 493:381–384

Kane SR, Ciardi DR, Gelino DM, von Braun K. 2012. *MNRAS* 425:757–762

Kasting JF, Whitmire DP, Reynolds RT. 1993. *Icarus* 101:108–128

Kennedy GM, Wyatt MC, Bryden G, Wittenmyer R, Sibthorpe B. 2013. *MNRAS* 436:898–903

- Kipping DM. 2013. *MNRAS* 434:L51–L55
- Kipping DM. 2014. *Proc. Frank N. Bash Symp. 2013: New Horizons in Astronomy*, Oct. 6–8, Austin, Tex. Austin: Univ. Tex.
- Kipping DM, Dunn WR, Jasinski JM, Manthri VP. 2012. *MNRAS* 421:1166–1188
- Konacki M, Wolszczan A. 2003. *Ap. J. Let.* 591:L147–L150
- Kopparapu RK. 2013. *Ap. J. Let.* 767:L8
- Kostov VB, McCullough PR, Hinse TC, Tsvetanov ZI, Hébrard G, et al. 2013. *Ap. J.* 770:52
- Kraft RP. 1967. *Ap. J.* 150:551
- Lafrenière D, Doyon R, Marois C, Nadeau D, Oppenheimer BR, et al. 2007. *Ap. J.* 670:1367–1390
- Lagrange AM, Boccaletti A, Milli J, Chauvin G, Bonnefoy M, et al. 2012. *Astron. Astrophys.* 542:A40
- Lagrange AM, Bonnefoy M, Chauvin G, Apai D, Ehrenreich D, et al. 2010. *Science* 329:57
- Lai D, Foucart F, Lin DNC. 2011. *MNRAS* 412:2790–2798
- Lai D. 2012. *MNRAS* 423:486–492
- Latham DW. 2012. *New Astron. Rev.* 56:16–18
- Latham DW, Rowe JF, Quinn SN, Batalha NM, Borucki WJ, et al. 2011. *Ap. J. Let.* 732:L24
- Laughlin G, Chambers J, Fischer D. 2002. *Ap. J.* 579:455–467
- Le Bouquin JB, Absil O, Benisty M, Massi F, Mérand A, Stefl S. 2009. *Astron. Astrophys.* 498:L41–L44
- Lee MH, Peale SJ. 2002. *Ap. J.* 567:596–609
- Limbach MA, Turner EL. 2014. *Proc. Nat. Acad. Sci.* 112:20–24
- Lin DNC, Bodenheimer P, Richardson DC. 1996. *Nature* 380:606–607
- Lissauer JJ. 2012. *New Astron. Rev.* 56:1–1
- Lissauer JJ, Jontof-Hutter D, Rowe JF, Fabrycky DC, Lopez ED, et al. 2013. *Ap. J.* 770:131
- Lissauer JJ, Ragozzine D, Fabrycky DC, Steffen JH, Ford EB, et al. 2011. *Ap. J. Suppl.* 197:8
- Lithwick Y, Xie J, Wu Y. 2012. *Ap. J.* 761:122
- Lloyd JP. 2011. *Ap. J. Let.* 739:L49
- Macintosh B, Graham JR, Ingraham P, Konopacky Q, Marois C, et al. 2014. *Proc. Nat. Acad. Sci.*, 111:12661
- Mahadevan S, Ramsey L, Bender C, Terrien R, Wright JT, et al. 2012. In *Ground-Based and Airborne Instrumentation for Astronomy IV*, ed. IS McLean, SK Ramsay, H Takami. *Proc. SPIE Conf. Ser.* 8446:84461S. Bellingham, WA: SPIE
- Marcy GW, Butler RP. 2000. *Pub. Astron. Soc. Pac.* 112:137–140
- Marcy GW, Isaacson H, Howard AW, Rowe JF, Jenkins JM, et al. 2014. *Ap. J. Suppl.* 210:20
- Mardling RA. 2007. *MNRAS* 382:1768–1790
- Marois C, Zuckerman B, Konopacky QM, Macintosh B, Barman T. 2010. *Nature* 468:1080–1083
- Martin DV, Triaud AHMJ. 2014. *Astron. & Astroph.* 570:91
- Masuda K. 2014. *Ap. J.* 783:53
- Matthews B, Kennedy G, Sibthorpe B, Booth M, Wyatt M, et al. 2014. *Ap. J.* 780:97
- Mayor M, Marmier M, Lovis C, Udry S, Ségransan D, et al. 2011. Submitted to *Astron. & Astroph.*, [arxiv:1109.2497](https://arxiv.org/abs/1109.2497)
- Mazeh T, Holczer T, Shporer A. 2015. *Ap. J.* 800:142
- Mazeh T, Krymolowski Y, Rosenfeld G. 1997. *Ap. J. Let.* 477:L103–L106
- Mazeh T, Shaham J. 1979. *Astron. Astrophys.* 77:145–151
- Mazeh T, Perets H, McQuillan A, Goldstein E. 2014. *Ap. J.* 801:3
- McArthur BE, Benedict GF, Barnes R, Martioli E, Korzennik S, et al. 2010. *Ap. J.* 715:1203–1220
- McQuillan A, Mazeh T, Aigrain S. 2013. *Ap. J. Let.* 775:L11
- Mizuno H. 1980. *Progress of Theoretical Physics* 64:544–557
- Moorhead AV, Ford EB, Morehead RC, Rowe J, Borucki WJ, et al. 2011. *Ap. J. Suppl.* 197:1
- Morton TD, Winn JN. 2014. *Ap. J.* 796:47
- Mudryk LR, Wu Y. 2006. *Ap. J.* 639:423–431
- Mugrauer M, Ginski C, Seeliger M. 2014. *MNRAS* 439:1063–1070

- Mulders GD, Pascucci I, Apai D. 2014. *Ap. J.* 798:112
- Naef D, Latham DW, Mayor M, Mazeh T, Beuzit JL, et al. 2001. *Astron. Astrophys.* 375:L27–L30
- Naoz S, Farr WM, Lithwick Y, Rasio FA, Teyssandier J. 2011. *Nature* 473:187–189
- Nelson BE, Ford EB, Wright JT, Fischer DA, von Braun K, et al. 2014. *MNRAS* 441:442–451
- Nesvorný D, Kipping D, Terrell D, Feroz F. 2014. *Ap. J.* 790:31
- Nesvorný D, Kipping D, Terrell D, Hartman J, Bakos GÁ, Buchhave LA. 2013. *Ap. J.* 777:3
- Nesvorný D, Kipping DM, Buchhave LA, Bakos GÁ, Hartman J, Schmitt AR. 2012. *Science* 336:1133
- Nielsen EL, Close LM. 2010. *Ap. J.* 717:878–896
- Nielsen EL, Liu MC, Wahhaj Z, Biller BA, Hayward TL, et al. 2014. *Ap. J.*, 794:158
- Nutzman P, Charbonneau D. 2008. *Pub. Astron. Soc. Pac.* 120:317–327
- Nutzman PA, Fabrycky DC, Fortney JJ. 2011. *Ap. J. Let.* 740:L10
- Ogilvie GI. 2014. *Annu. Rev. Astron. Astrophys.* 52:171–210
- Orosz JA, Welsh WF, Carter JA, Brugamyer E, Buchhave LA, et al. 2012a. *Ap. J.* 758:87
- Orosz JA, Welsh WF, Carter JA, Fabrycky DC, Cochran WD, et al. 2012b. *Science* 337:1511
- Park BG, Kim SL, Lee JW, Lee BC, Lee CU, et al. 2012. In *Ground-Based and Airborne Telescopes I*, ed. LM Stepp, R Gilmozzi, HJ Hall. *Proc. SPIE Conf. Ser.* 8444:844447. Bellingham, WA: SPIE
- Pasquini L, Avila G, Dekker H, Delabre B, D’Odorico S, et al. 2008. In *Ground-Based and Airborne Instrumentation for Astronomy II*, ed. IS McLean, MM Casali. *Proc. SPIE Conf. Ser.* 7014:70141I. Bellingham, WA: SPIE
- Pepe FA, Cristiani S, Rebolo Lopez R, Santos NC, Amorim A, et al. 2010. In *Ground-Based and Airborne Instrumentation for Astronomy III*, ed. IS McLean, SK Ramsay, H Takami. *Proc. SPIE Conf. Ser.* 7735:77350F. Bellingham, WA: SPIE
- Pepper J, Gould A, Depoy DL. 2003. *Acta Astronomica* 53:213–228
- Petigura EA, Howard AW, Marcy GW. 2013. *Proc. Nat. Acad. Sci.* 110:19273
- Pierens A, Nelson RP. 2008. *Astron. Astrophys.* 483:633–642
- Plavchan P, Bilinski C, Currie T. 2014. *Publ. Astron. Soc. Pacific* 126:34–47
- Pollack JB, Hubickyj O, Bodenheimer P, Lissauer JJ, Podolak M, Greenzweig Y. 1996. *Icarus* 124:62–85
- Pont F. 2009. *MNRAS* 396:1789–1796
- Poppenhaeager K, Wolk SJ. 2014. *Astron. Astrophys.* 565:L1
- Pourbaix D, Tokovinin AA, Batten AH, Fekel FC, Hartkopf WI, et al. 2004. *Astron. Astrophys.* 424:727–732
- Pravdo SH, Shaklan SB. 2009. *Ap. J.* 700:623–632
- Queloz D, Eggenberger A, Mayor M, Perrier C, Beuzit JL, et al. 2000. *Astron. Astrophys.* 359:L13–L17
- Quirrenbach A, Amado PJ, Mandel H, Caballero JA, Mundt R, et al. 2010. In *Ground-Based and Airborne Instrumentation for Astronomy III*, ed. IS McLean, SK Ramsay, H Takami. *Proc. SPIE Conf. Ser.* 7735:773513. Bellingham, WA: SPIE
- Raghavan D, McAlister HA, Henry TJ, Latham DW, Marcy GW, et al. 2010. *Ap. J. Suppl.* 190:1–42
- Rappaport S, Sanchis-Ojeda R, Rogers LA, Levine A, Winn JN. 2013. *Ap. J. Let.* 773:L15
- Rasio FA, Ford EB. 1996. *Science* 274:954–956
- Rauer H, Catala C, Aerts C, Appourchaux T, Benz W, et al. 2014. *Experimental Astronomy*, 41
- Raymond SN, Barnes R, Mandell AM. 2008. *MNRAS* 384:663–674
- Reggiani M, Quanz SP, Meyer MR, Pueyo L, Absil O, et al. 2014. *Ap. J. Let.* 792:L23
- Ricker GR, Winn JN, Vanderspek R, Latham DW, Bakos GÁ, et al. 2014. *Journal of Astronomical Telescopes, Instruments, and Systems* 1:014003
- Rivera EJ, Laughlin G, Butler RP, Vogt SS, Haghighipour N, Meschiari S. 2010. *Ap. J.* 719:890–899
- Rivera EJ, Lissauer JJ. 2001. *Ap. J.* 558:392–402
- Roell T, Neuhäuser R, Seifahrt A, Mugrauer M. 2012. *Astron. Astrophys.* 542:A92
- Rogers TM, Lin DNC, Lau HHB. 2012. *Ap. J. Let.* 758:L6

- Roy AE, Ovenden MW. 1954. *MNRAS* 114:232
- Sahlmann J, Ségransan D, Queloz D, Udry S, Santos NC, et al. 2011. *Astron. Astrophys.* 525:A95
- Sanchis-Ojeda R, Fabrycky DC, Winn JN, Barclay T, Clarke BD, et al. 2012. *Nature* 487:449–453
- Sanchis-Ojeda R, Rappaport S, Winn JN, Kotson MC, Levine A, El Mellah I. 2014. *Ap. J.* 787:47
- Sanchis-Ojeda R, Winn JN, Holman MJ, Carter JA, Osip DJ, Fuentes CI. 2011. *Ap. J.* 733:127
- Santos NC, Israelian G, Mayor M. 2004. *Astron. Astrophys.* 415:1153–1166
- Schlaufman KC. 2010. *Ap. J.* 719:602–611
- Schlaufman KC. 2014. *Ap. J.* 790:91
- Schlaufman KC, Winn JN. 2013. *Ap. J.* 772:143
- Schneider J. 1994. *Planetary and Space Science* 42:539–544
- Schneider J, Dedieu C, Le Sidaner P, Savalle R, Zolotukhin I. 2011. *Astron. Astrophys.* 532:A79
- Schwamb ME, Orosz JA, Carter JA, Welsh WF, Fischer DA, et al. 2013. *Ap. J.* 768:127
- Seager S, ed. 2011. *Exoplanets*. University of Arizona Press (Tucson, AZ)
- Seager S. 2013. *Science* 340:577–581
- Shen Y, Turner EL. 2008. *Ap. J.* 685:553–559
- Sigurdsson S, Stairs IH, Moody K, Arzoumanian KMZ, Thorsett SE. 2008. In *Extreme Solar Systems*, ed. D Fischer, FA Rasio, SE Thorsett, A Wolszczan. *ASP Conf. Ser.* 398:119. San Francisco: ASP
- Silburt A, Gaidos E, Wu Y. 2015. *Ap. J.* 799:180
- Sliski DH, Kipping DM. 2014. *Ap. J.* 788:148
- Snellen IAG, Brandl BR, de Kok RJ, Brogi M, Birkby J, Schwarz H. 2014. *Nature* 509:63–65
- Sousa SG, Santos NC, Mayor M, Udry S, Casagrande L, et al. 2008. *Astron. Astrophys.* 487:373–381
- Steffen JH, Farr WM. 2013. *Ap. J. Let.* 774:L12
- Steffen JH, Ragozzine D, Fabrycky DC, Carter JA, Ford EB, et al. 2012. *Proceedings of the National Academy of Science* 109:7982–7987
- Storch NI, Anderson KR, Lai D. 2014. *Science* 345:1317
- Sumi T, Kamiya K, Bennett DP, Bond IA, Abe F, et al. 2011. *Nature* 473:349–352
- Szabó GM, Szabó R, Benkő JM, Lehmann H, Mező G, et al. 2011. *Ap. J. Let.* 736:L4
- Szentgyorgyi A, Frebel A, Furesz G, Hertz E, Norton T, et al. 2012. In *Ground-Based and Airborne Instrumentation for Astronomy IV*, ed. IS McLean, SK Ramsay, H Takami. *Proc. SPIE Conf. Ser.* 8446:84461H. Bellingham, WA: SPIE
- Tamura M, Suto H, Nishikawa J, Kotani T, Sato B, et al. 2012. In *Ground-Based and Airborne Instrumentation for Astronomy IV*, ed. IS McLean, SK Ramsay, H Takami. *Proc. SPIE Conf. Ser.* 8446:84461T. Bellingham, WA: SPIE
- Tamuz O, Ségransan D, Udry S, Mayor M, Eggenberger A, et al. 2008. *Astron. Astrophys.* 480:L33–L36
- Tan X, Payne MJ, Lee MH, Ford EB, Howard AW, et al. 2013. *Ap. J.* 777:101
- Tarter JC, Backus PR, Mancinelli RL, Aurnou JM, Backman DE, et al. 2007. *Astrobiology* 7:30–65
- Teitler S, Königl A. 2014. *Ap. J.* 786:139
- Terquem C, Papaloizou JCB. 2007. *Ap. J.* 654:1110–1120
- Thebault P, Haghighipour N. 2014. In *Planetary Exploration and Science: Recent Advances and Applications*, ed. S Jin, N Haghighipour, WH Ip. Dordrecht, Neth.: Springer, pp. 309–340
- Thies I, Kroupa P, Goodwin SP, Stamatellos D, Whitworth AP. 2011. *MNRAS* 417:1817–1822
- Thommes EW, Lissauer JJ. 2003. *Ap. J.* 597:566–580
- Thorsett SE, Arzoumanian Z, Camilo F, Lyne AG. 1999. *Ap. J.* 523:763–770
- Traub WA. 2012. *Ap. J.* 745:20
- Tremaine S 1991. *Icarus* 89:85–92
- Tremaine S, Dong S. 2012. *Astron. J.* 143:94
- TriAUD AHMJ, Collier Cameron A, Queloz D, Anderson DR, Gillon M, et al. 2010. *Astron. Astrophys.* 524:A25
- Udry S, Mayor M, Naef D, Pepe F, Queloz D, et al. 2002. *Astron. Astrophys.* 390:267–279
- Udry S, Mayor M, Santos NC. 2003. *Astron. Astrophys.* 407:369–376



Valenti JA, Fischer DA. 2005. *Ap. J. Suppl.* 159:141–166

Valsecchi F, Rasio FA. 2014. *Ap. J.* 786:102

van Eyken JC, Ciardi DR, von Braun K, Kane SR, Plavchan P, et al. 2012. *Ap. J.* 755:42

Van Eylen V, Lund MN, Silva V, et al. 2014. *Ap. J.* 782:14

Veras D, Armitage PJ. 2004. *Icarus* 172:349–371

Veras D, Crepp JR, Ford EB. 2009. *Ap. J.* 696:1600–1611

Veras D, Ford EB. 2012. *MNRAS* 420:L23–L27

Veras D, Ford EB, Payne MJ. 2011. *Ap. J.* 727:74

Villaver E, Livio M. 2009. *Ap. J. Let.* 705:L81–L85

Walkowicz LM, Basri GS. 2013. *MNRAS* 436:1883–1895

Wang J, Fischer DA, Xie JW, Ciardi DR. 2014. *Ap. J.* 791:111

Wang J, Ford EB. 2011. *MNRAS* 418:1822–1833

Ward WR. 1997. *Icarus* 126:261–281

Watson CA, Littlefair SP, Diamond C, Collier Cameron A, Fitzsimmons A, et al. 2011. *MNRAS* 413:L71–L75

Weidenschilling SJ, Marzari F. 1996. *Nature* 384:619–621

Welsh WF, Orosz JA, Carter JA, Fabrycky DC, Ford EB, et al. 2012. *Nature* 481:475–479

Welsh WF, Orosz JA, Short DR, Haghighipour N, Buchhave LA, et al. 2014. Submitted to *Ap. J.*, [arxiv:1409.1605](https://arxiv.org/abs/1409.1605)

Wheatley PJ, Pollacco DL, Queloz D, Rauer H, Watson CA, et al. 2013. In *Eur. Phys. J. Web Conf.*, 47:13002

Williams IP, Cremin AW. 1968. *Q. Jl. R. Ast. Soc.* 9:40, p. 41

Winn JN, Fabrycky D, Albrecht S, Johnson JA. 2010. *Ap. J. Let.* 718:L145–L149

Winn JN, Johnson JA, Fabrycky D, Howard AW, Marcy GW, et al. 2009. *Ap. J.* 700:302–308

Winn JN, Johnson JA, Marcy GW, Butler RP, Vogt SS, et al. 2006. *Ap. J. Let.* 653:L69–L72

Wittenmyer RA, Endl M, Cochran WD, Levison HF, Henry GW. 2009. *Ap. J. Suppl.* 182:97–119

Wolszczan A, Frail DA. 1992. *Nature* 355:145–147

Wright DJ, Chené AN, De Cat P, Marois C, Mathias P, et al. 2011a. *Ap. J. Let.* 728:L20

Wright JT, Fakhouri O, Marcy GW, Han E, Feng Y, et al. 2011b. *Pub. Astron. Soc. Pac.* 123:412–422

Wright JT, Gaudi BS. 2013. In *Exoplanet Detection Methods*, eds. Oswalt TD, French LM, Kalas P., p. 489. Dordrecht, Neth: Springer

Wright JT, Marcy GW, Howard AW, Johnson JA, Morton TD, Fischer DA. 2012. *Ap. J.* 753:160

Wright JT, Upadhyay S, Marcy GW, Fischer DA, Ford EB, Johnson JA. 2009. *Ap. J.* 693:1084–1099

Wright JT, Veras D, Ford EB, Johnson JA, Marcy GW, et al. 2011c. *Ap. J.* 730:93

Wu Y, Lithwick Y. 2013. *Ap. J.* 772:74

Xiang-Gruess M, Papaloizou JCB. 2013. *MNRAS* 431:1320–1336

Xie JW, Wu Y, Lithwick Y. 2014. *Ap. J.* 789:165

Youdin AN. 2011. *Ap. J.* 742:38

Zakamska NL, Pan M, Ford EB. 2011. *MNRAS* 410:1895–1910

Zsom A, Seager S, de Wit J, Stamenković V. 2013. *Ap. J.* 778:109